Enhanced decay and line broadening of 2P *ortho*-positronium inside silica pores

Kenji Shu[1,2],

K. Yamada[2], K. Hashidate[2], A. Ishida[2], T. Namba[2], S. Asai[2],

M. Kuwata-Gonokami[2], Y. Tajima[1], E. Chae[1,7], K. Yoshioka[1],

N. Oshima[3], B.E. O'Rourke[3], K. Michishio[3], K. Ito[3], K. Kumagai[3],

R. Suzuki[3], S. Fujino[4], T. Hyodo[5], I. Mochizuki[5], K. Wada[5] and T. Kai[6]

[1]Photon Science Center (PSC) and Department of Applied Physics, Graduate School of Engineering, UTokyo

[2]Department of Physics, Graduate School of Science, and ICEPP, UTokyo

[3]AIST [4]Global Innovation Center (GIC), Kyushu University [5]IMSS, KEK [6]JAEA

[7]Department of Physics, College of Science, Korea University

12.5th International Workshop on Positron and Positronium Chemistry
Online

Interaction of Ps with matters has make Ps useful probe

Pick-off decay

Decay of Ps with an electron on the material surface

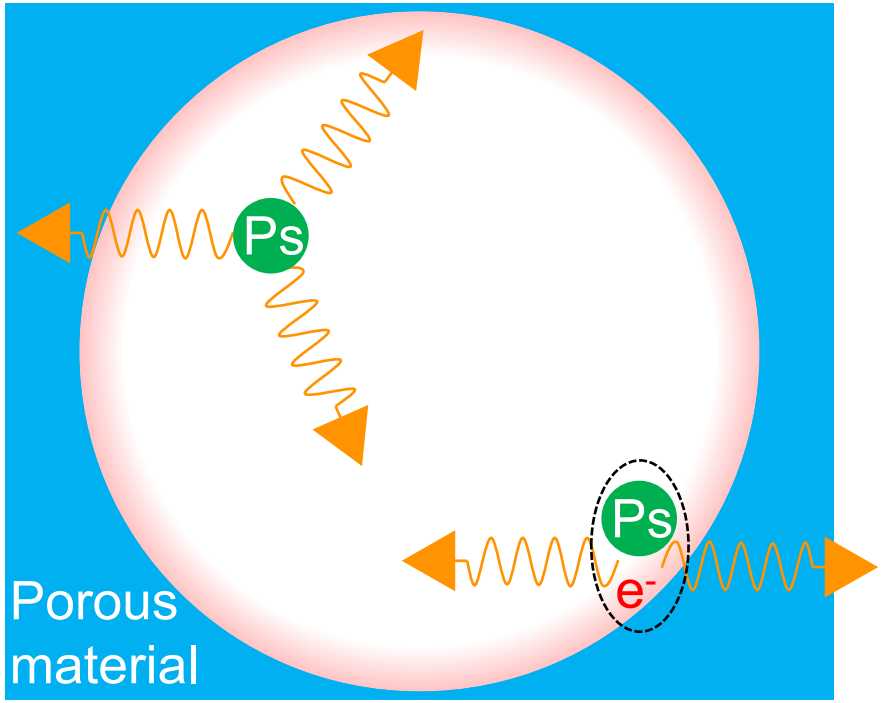

Can inspect porous structure such as pore sizes and porosities

Spin-conversion

o-Ps's spin-flip to short-lived *p*-Ps by paramagnetic centers

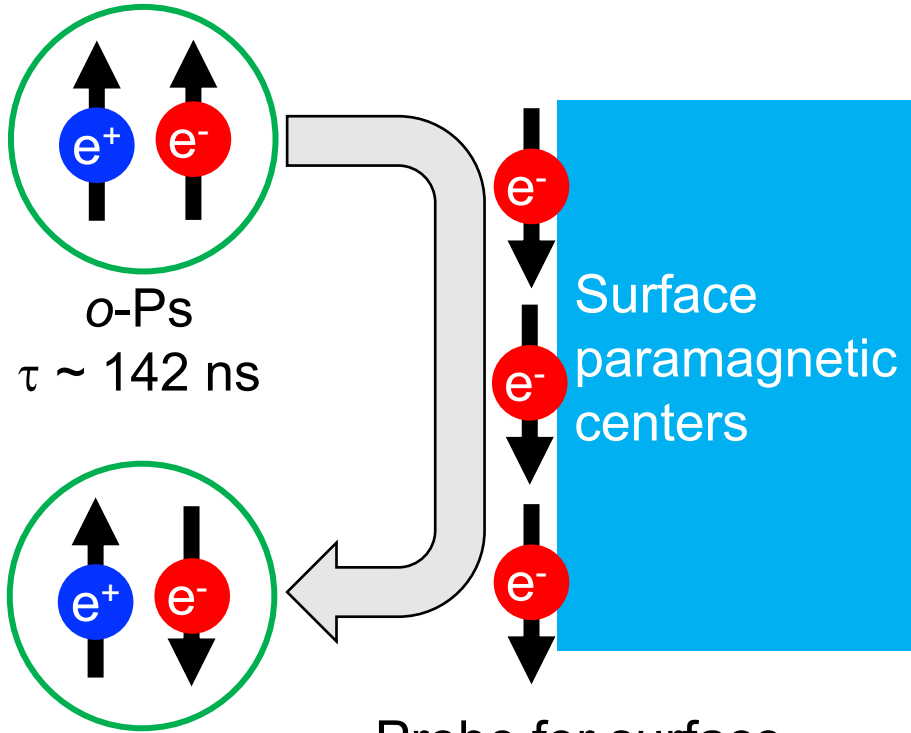

o-Ps
τ ~ 142 ns

p-Ps
τ ~ 125 ps

Probe for surface unpaired spin

Ps in its excited state exhibits another face

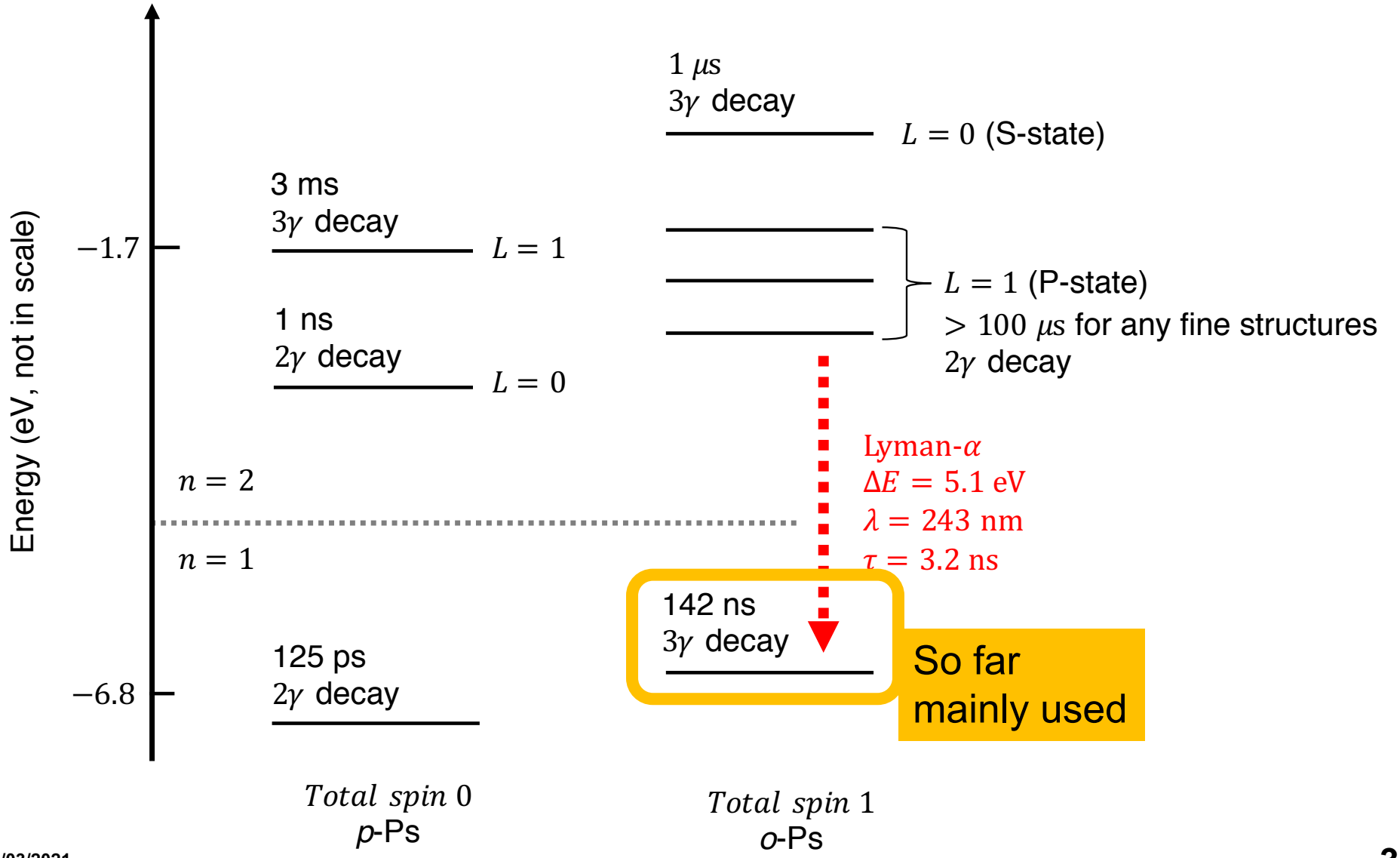

Ps in its excited state exhibits another face

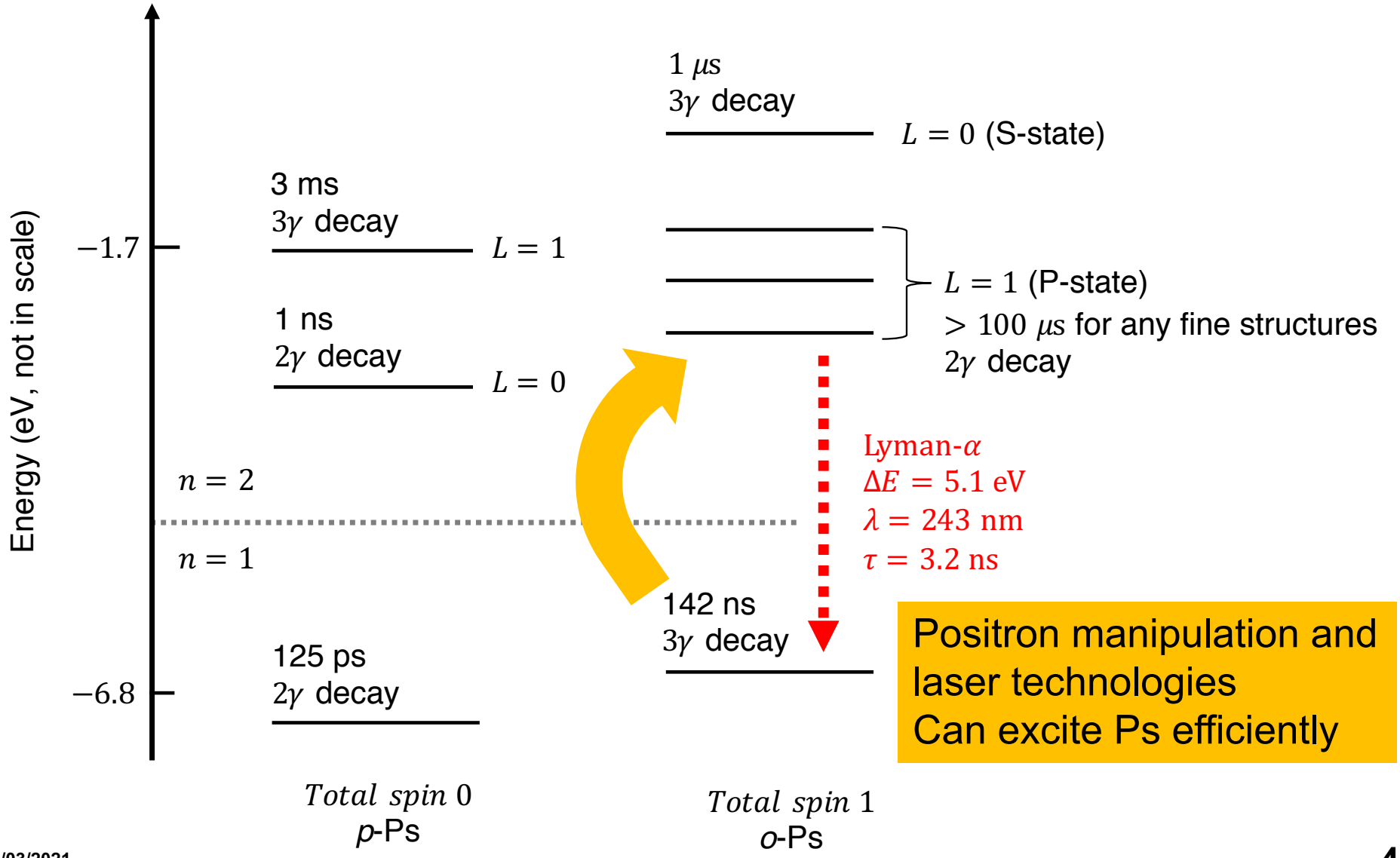

Positron manipulation and laser technologies
Can excite Ps efficiently

Unexplained rapid decay and line broadening have been discovered

Cooper *et al.*, Phys. Rev. B **97**, 205302 (2018) reported unexplained results in excitation into the 2P state

Rapid decay after excitation

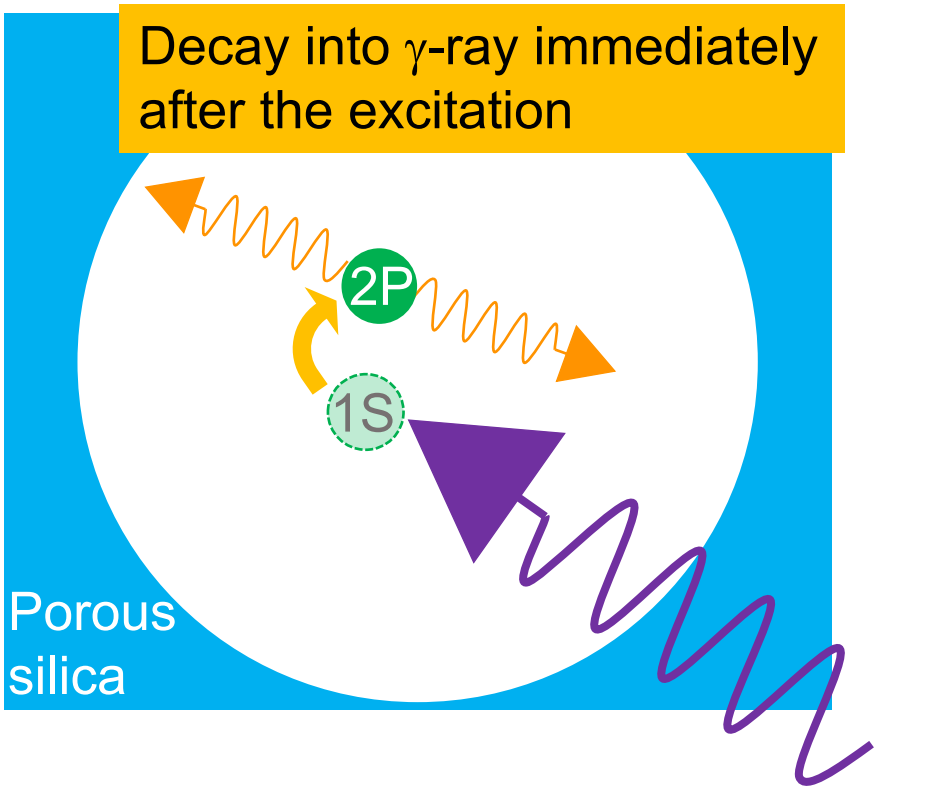

Line broadening

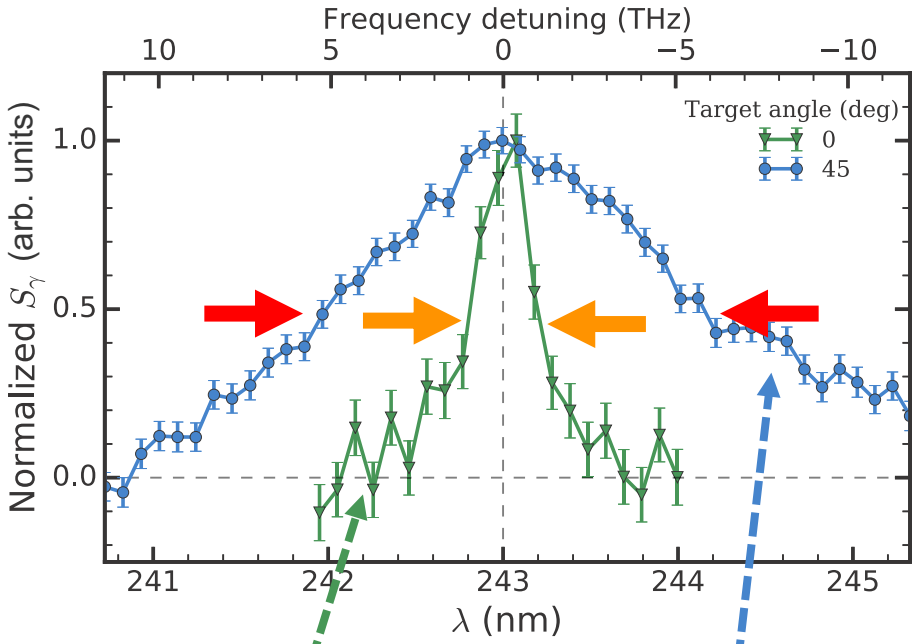

Cooper *et al.*, Phys. Rev. B **97**, 205302 (2018)

Doppler width for Ps in vacuum

Much wider reason?

To be a new way as material probe and Ps cooling for fundamental study

By understanding interactions between 2P-Ps and materials :

1. Use 2P-Ps as a new probe of material structure

In **some materials**, the unexplained result was **not** observed

Another porous silica

Cassidy et al.,
Phys. Rev. Lett. 106, 023401 (2011)

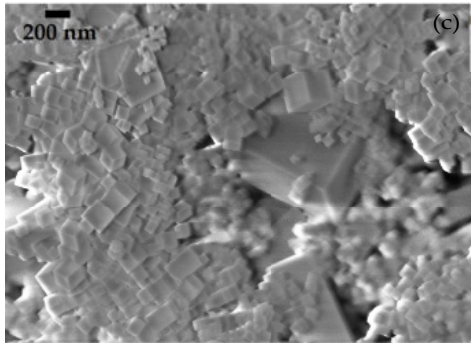

MgO smoke

Gurung *et al.*, Phys. Rev. A 101, 012701 (2020)

2P-Ps should respond some structures in material. **Probe it!**

2. Enable rapid Ps cooling combining with laser cooling

- Laser cooling on Ps in porous silica will be effective
  Shu *et al.*, J. Phys. B: At. Mol. Opt. Phys. **49**, 104001 (2016)
- Breakthrough to Ps-BEC, precise spectroscopy
- Please refer talks by A. Ishida, R. Uozumi, Y. Tajima on August 31
- Suppressing the unexplained results is necessary

Contaminants are trapping Ps?

In Cooper *et al.*, Phys. Rev. B **97**, 205302 (2018), contaminants on pore surface were suspected

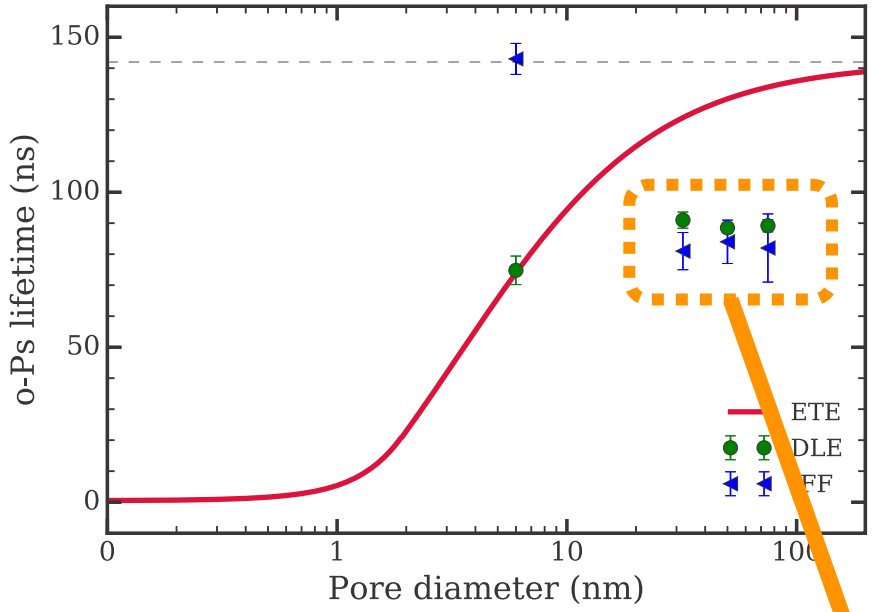

Cooper *et al.*, Phys. Rev. B **97**, 205302 (2018)

Not valid?

- In their nano pores, 1S o-Ps lifetimes were much shorter than predictions by RTE model

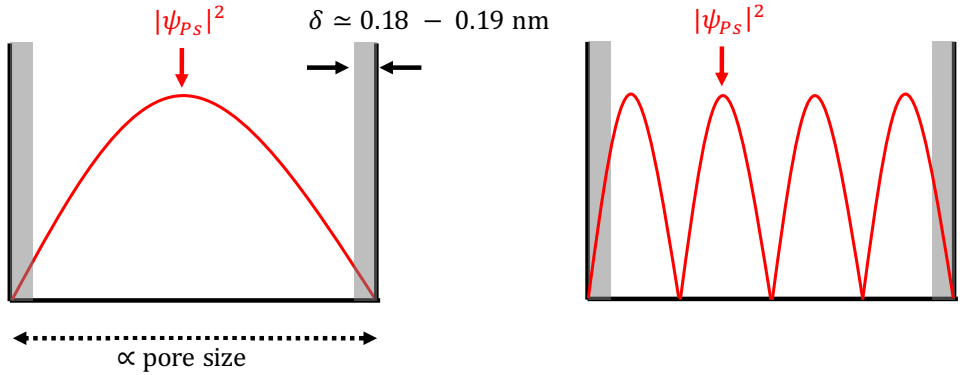

Predicts pick-off decay rate quantitatively

- Ps has the wavefunction in infinite squared well
- Ps has a large annihilation rate in the vicinity of the surface

Contaminants are trapping Ps?

In Cooper *et al.*, Phys. Rev. B **97**, 205302 (2018), contaminants on pore surface were suspected

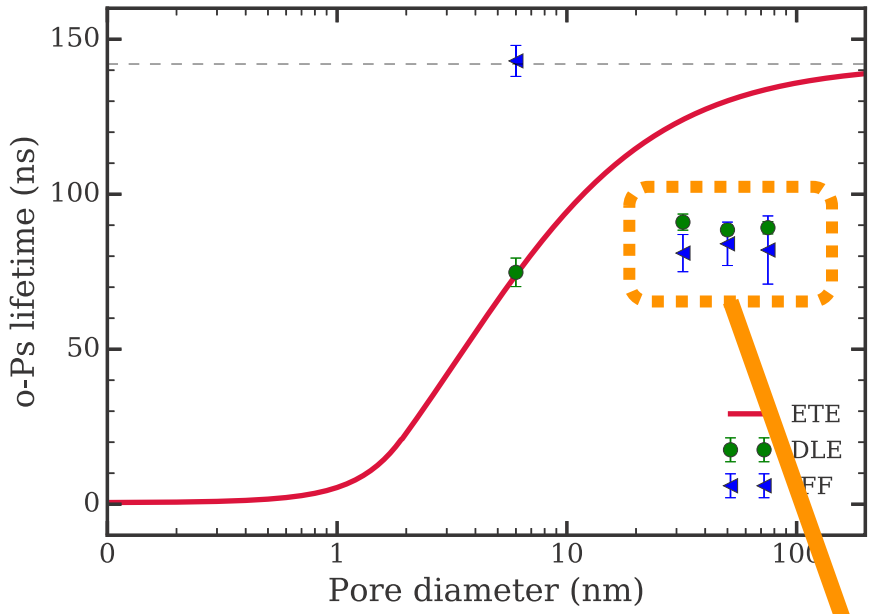

Cooper *et al.*, Phys. Rev. B **97**, 205302 (2018)

- In their nano pores, 1S o-Ps lifetimes were much shorter than predictions by RTE model

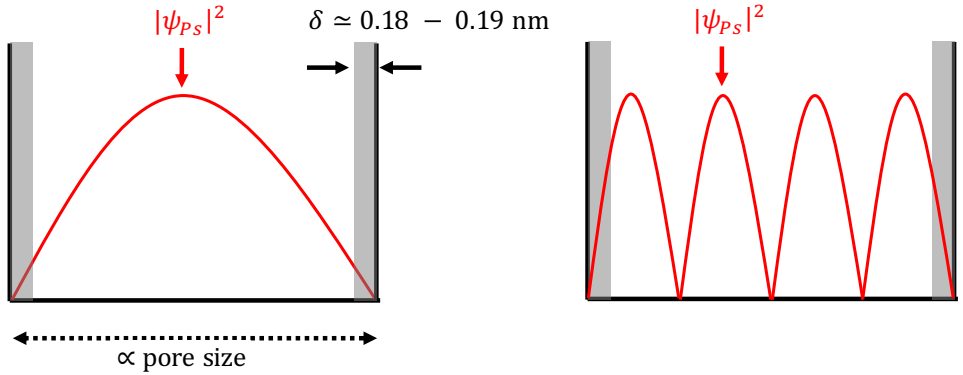

Not valid?

Predicts pick-off decay rate quantitatively

- Ps has the wavefunction in infinite

1. test this hypothesis
2. study basic properties of these phenomena

tion rate in the vicinity of the surface

Experiments at KEK-SPF

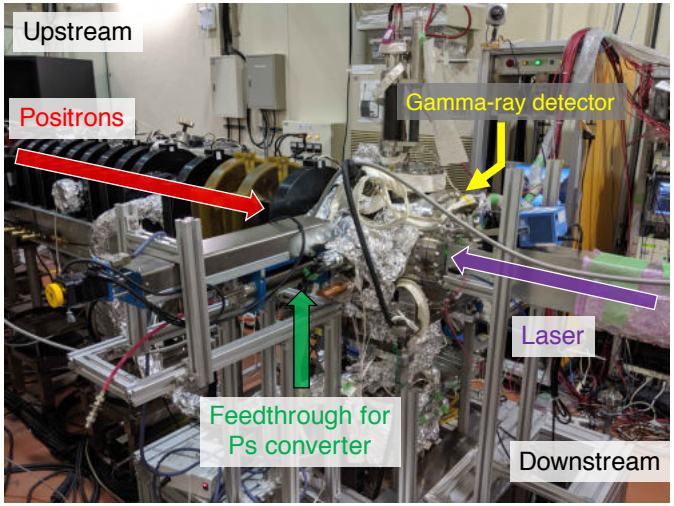

Figure 2.1: Picture of the experimental setup.

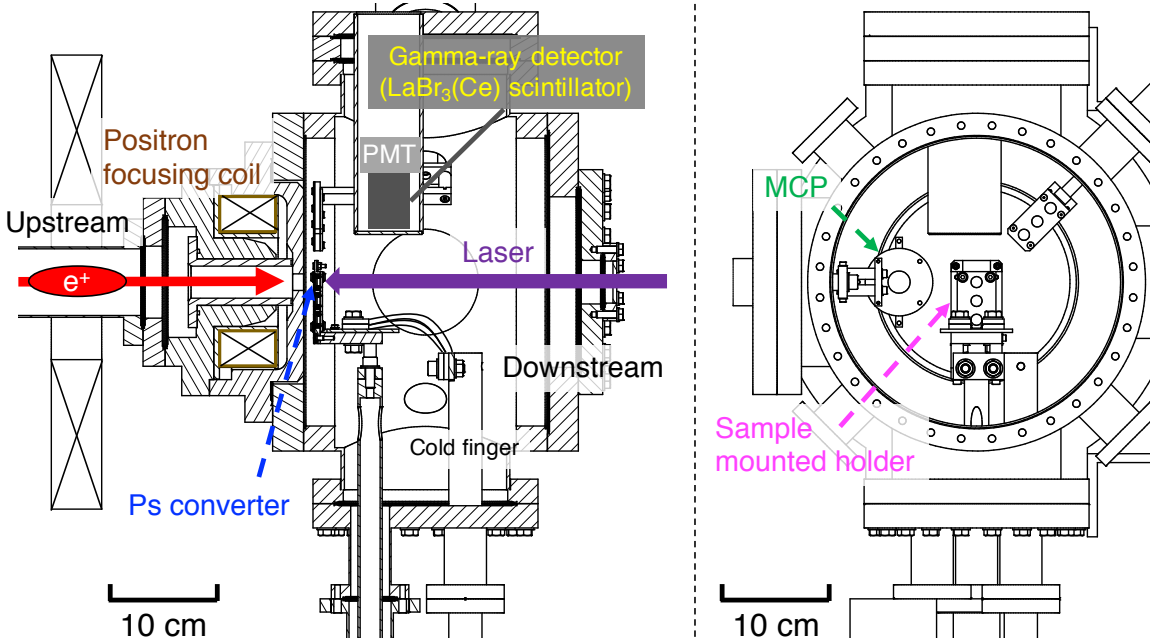

Figure 2.2: Drawings of the experimental chamber to excite Ps confined in the Ps converter.

- KEK-SPF can provide bunched slow positron beam
- Silica aerogel was used as a Ps converter and trap
- UV nano-second pulsed laser was synchronized

Bunched positrons produce a lot of γ-rays detected with pileup

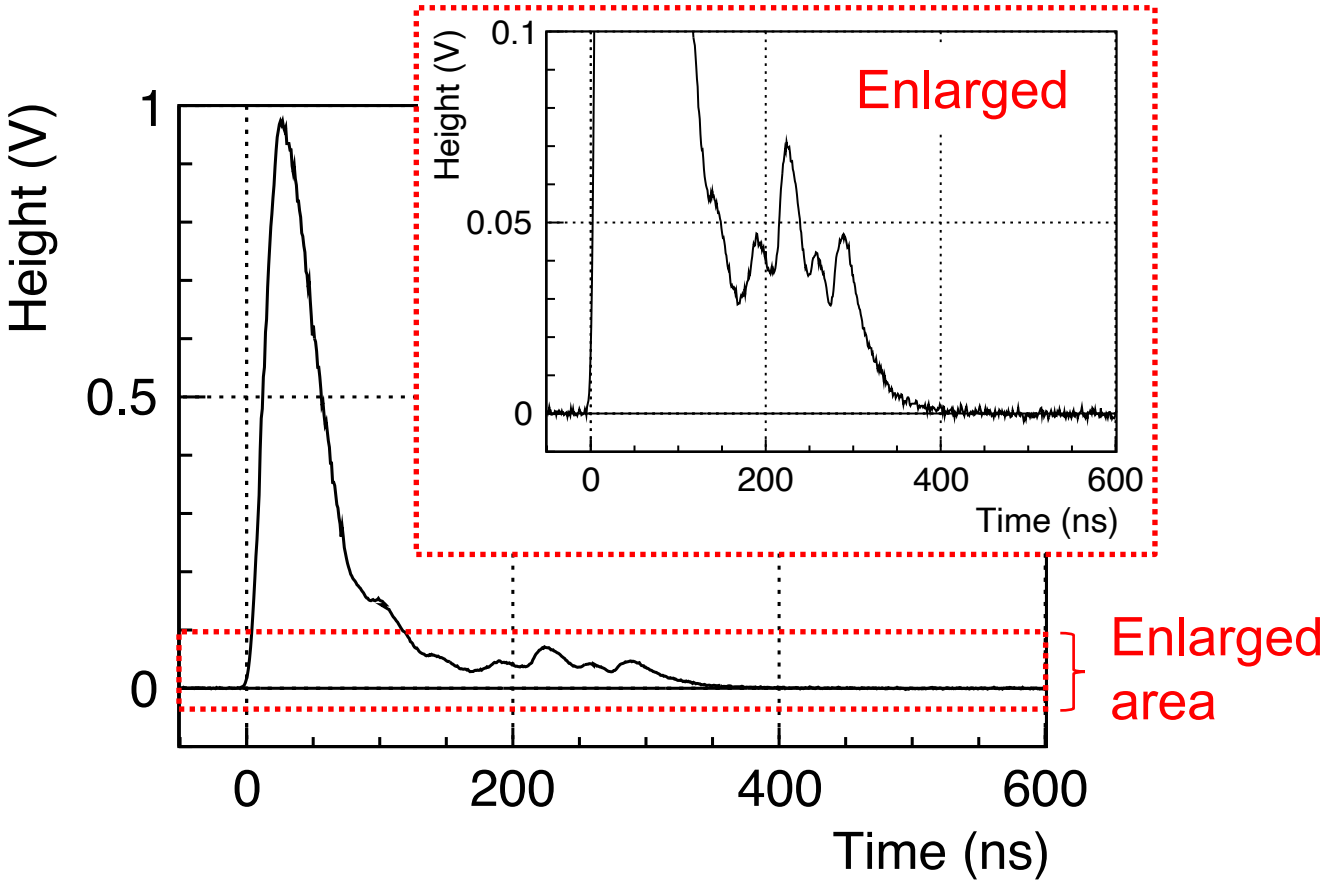

Typical PMT waveform which detected γ-rays

We adopt the SSPALS method

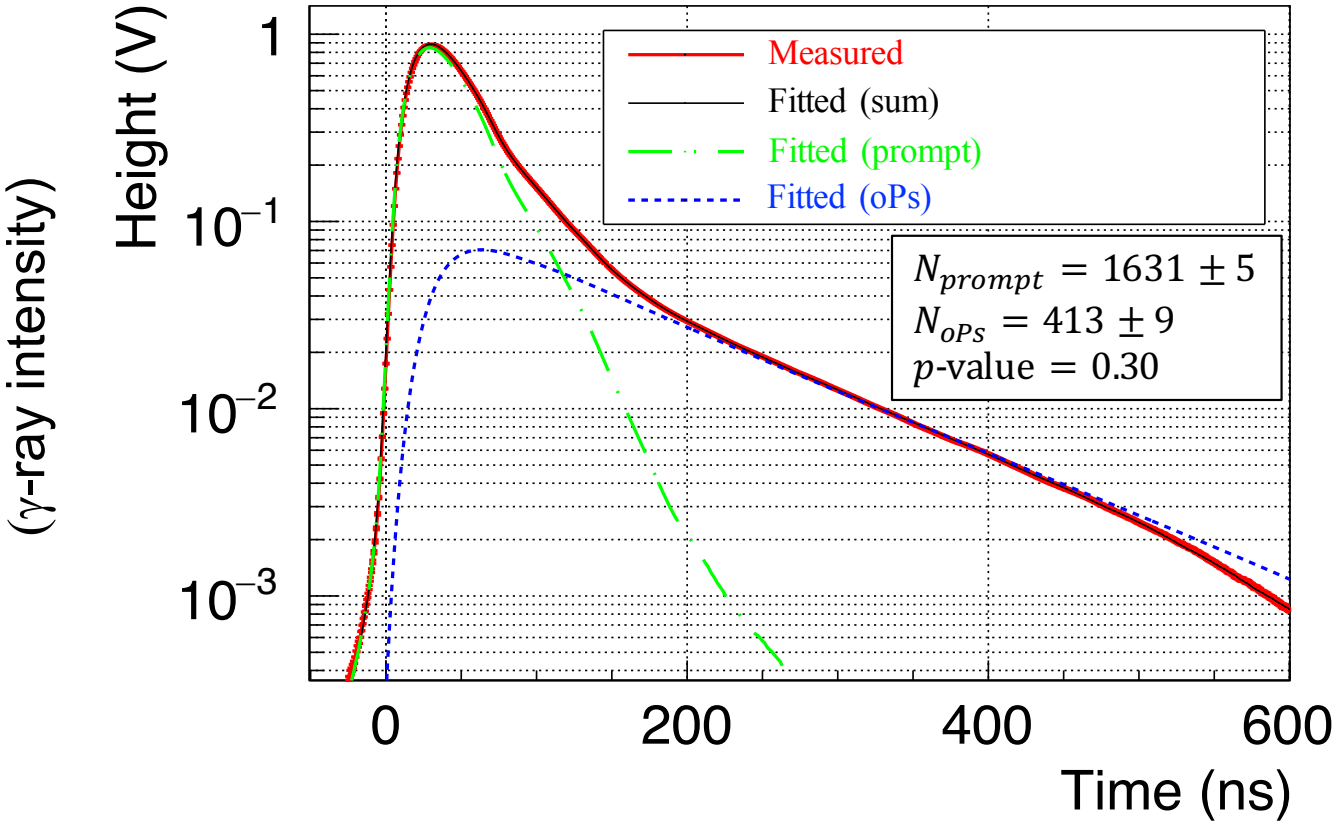

Measured average waveform and fitted function

Averaged waveforms over bunches were analyzed with a modeled function including Ps lifetime and intensity

Lifetime of 1S *o*-Ps agreed with the RTE model prediction

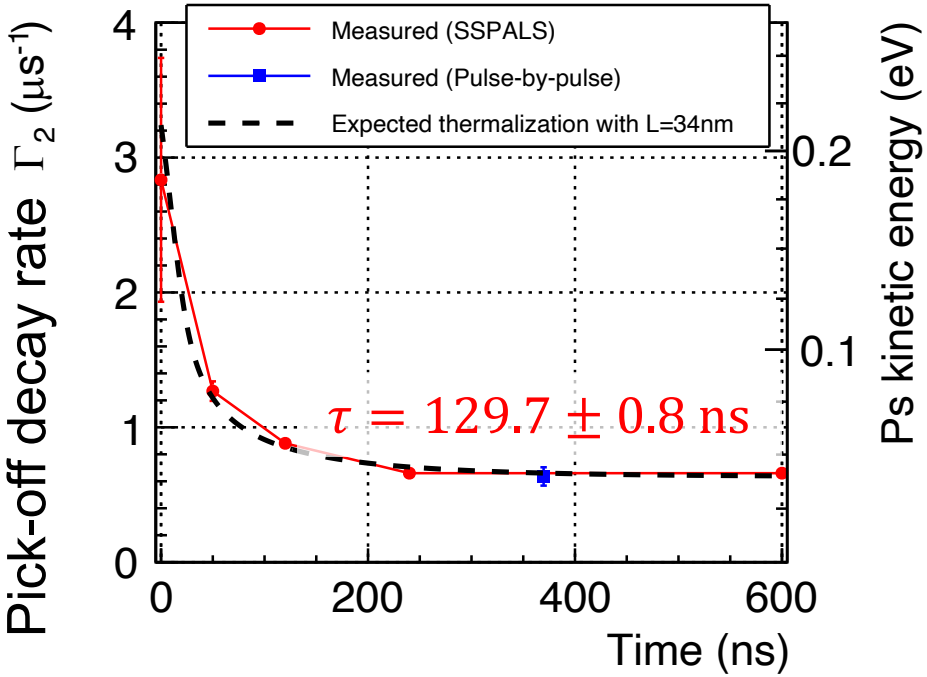

In our aerogel :
D = 50 nm, τ ~ 130 ns

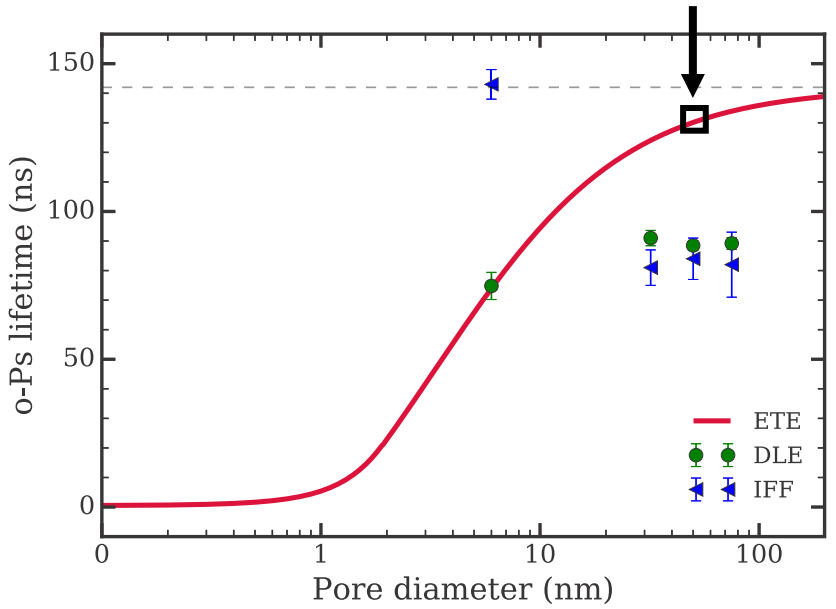

Cooper *et al.*, Phys. Rev. B **97**, 205302 (2018)

Thermalized lifetime was ~130 ns

Agreed with other methods including bulk-PALS measurement

Contaminants are much less than the previous work

Even with less contaminants, excitation induced the enhance decay

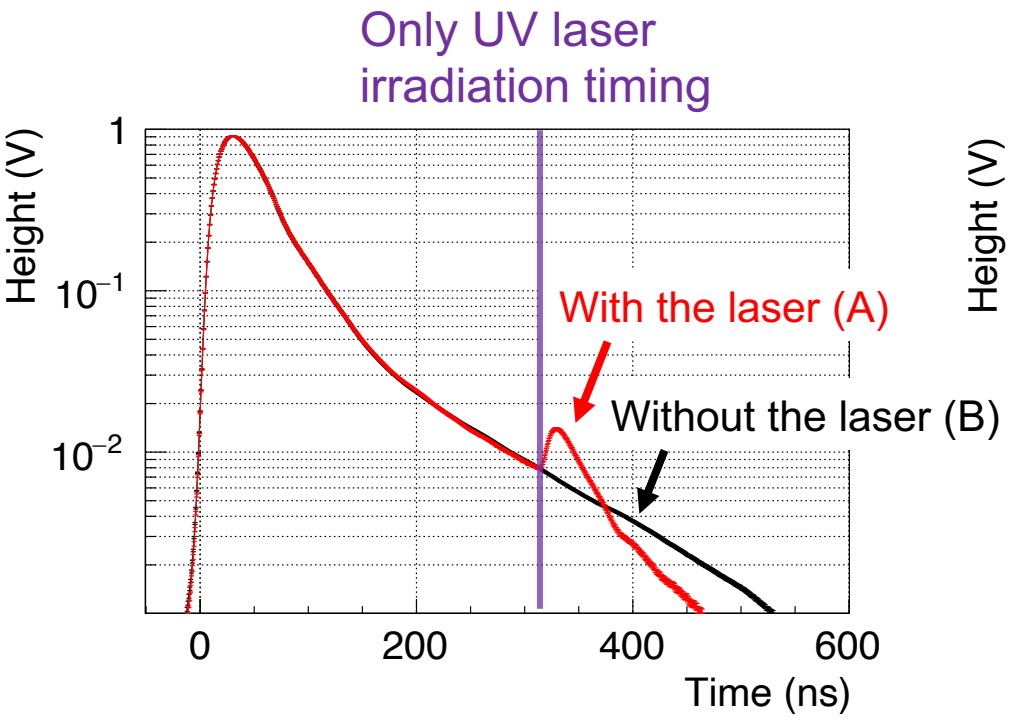

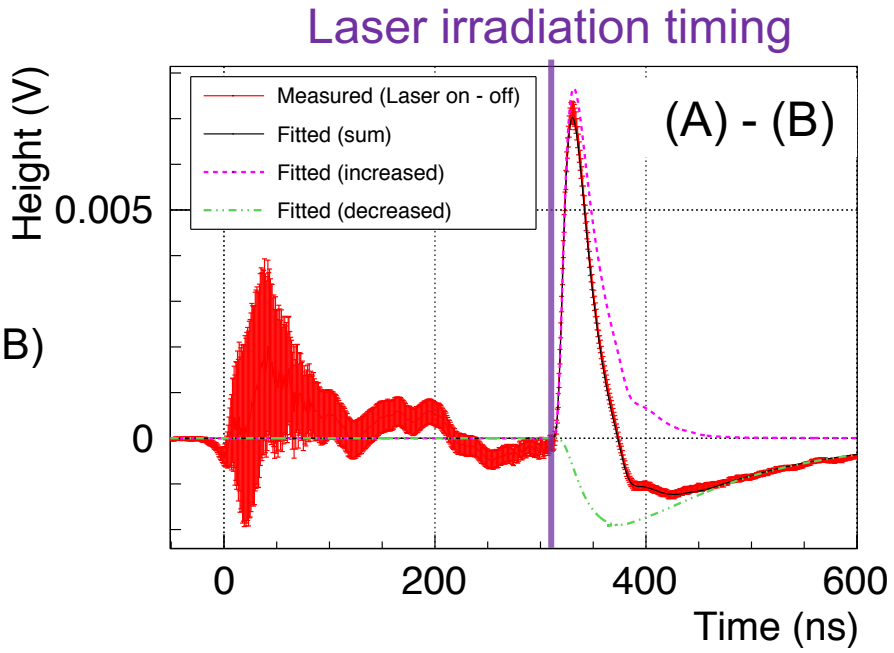

Waveform averages with / without laser

Difference by laser irradiation fitted by the following model

Laser excitation triggered enhanced decay into γ-rays

Quantitatively model the enhanced decay

To quantitatively study the unexplained result, we modeled the enhanced decay by the optical Bloch equation

Ps wavefunction : $|\Psi(t)\rangle = c_1(t)|1S\rangle + c_2(t)|2P\rangle, \qquad \rho_{ij} = c_i^* c_j$

$$\begin{cases} \dfrac{\mathrm{d}}{\mathrm{d}t}\rho_{11} = \dfrac{i}{2}\Omega(\rho_{12} - \rho_{21}) - \Gamma_1\rho_{11} + (\Gamma_{sp} + P_1\Gamma_2)\rho_{22}, \\ \dfrac{\mathrm{d}}{\mathrm{d}t}\rho_{12} = \dfrac{\mathrm{d}}{\mathrm{d}t}\rho_{21}^* = \dfrac{i}{2}\Omega(\rho_{11} - \rho_{22}) + \left(i(\omega_{21} - \omega_L) - \dfrac{1}{2}(\Gamma_1 + \Gamma_{\mathrm{sp}} + \Gamma_2)\right)\rho_{12}, \\ \dfrac{\mathrm{d}}{\mathrm{d}t}\rho_{22} = -\dfrac{i}{2}\Omega(\rho_{12} - \rho_{21}) - (\Gamma_{sp} + \Gamma_2)\rho_{22}. \end{cases}$$

Γ_2 is the enhanced decay rate of 2P Ps
By inputting laser parameters (pulse energy, wavelength),
we can calculate **Ps decay probability**

Estimated by fitting measured waveform

There should be inhomogeneous broadening

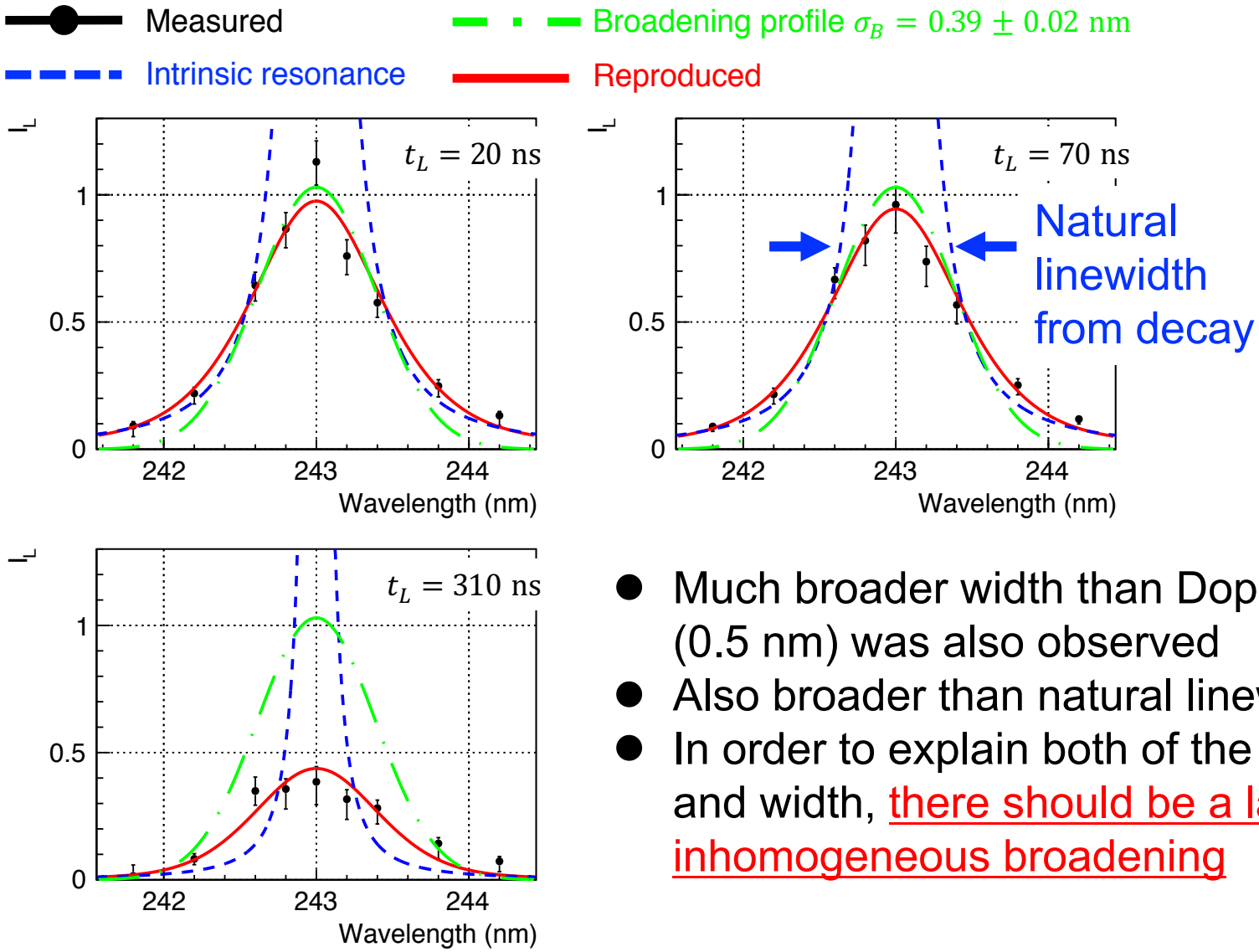

- Much broader width than Doppler (0.5 nm) was also observed
- Also broader than natural linewidth
- In order to explain both of the prob. and width, there should be a large inhomogeneous broadening

Distribution of Stark shift can cause inhomogeneous broadening

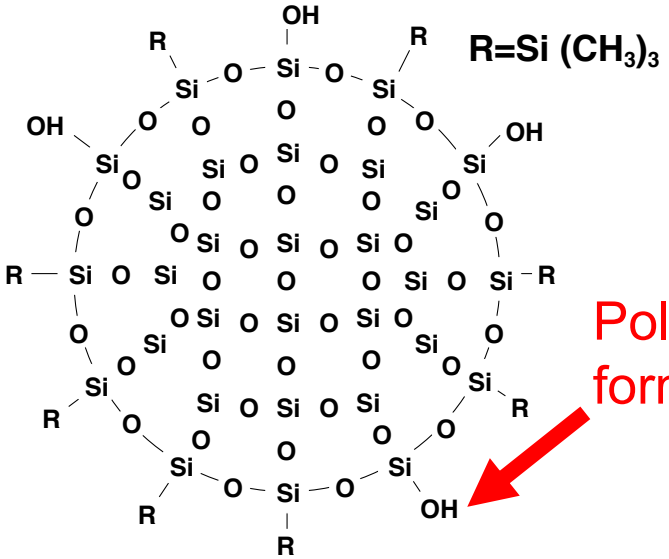

Structural diagram of silica grain

Y. Kataoka, PhD thesis (2007)

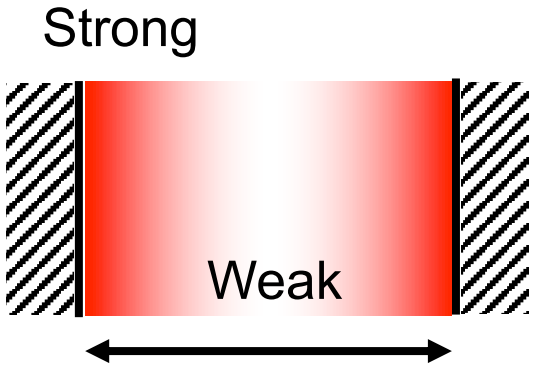

Inside a pore

Field strength distribute against distance from surface

- Electric field shifts Ps energy, then resonant wavelength
- Field distribution cause broadening
- Field inside aerogel pore can be strong enough to cause the observed broadening

0.02 eV = 1 nm of 243 nm

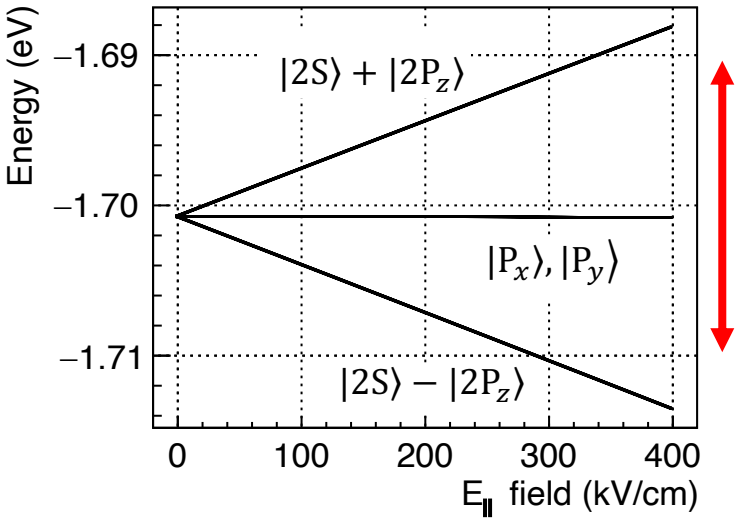

Enhanced decay rate had positive correlation with kinetic energy

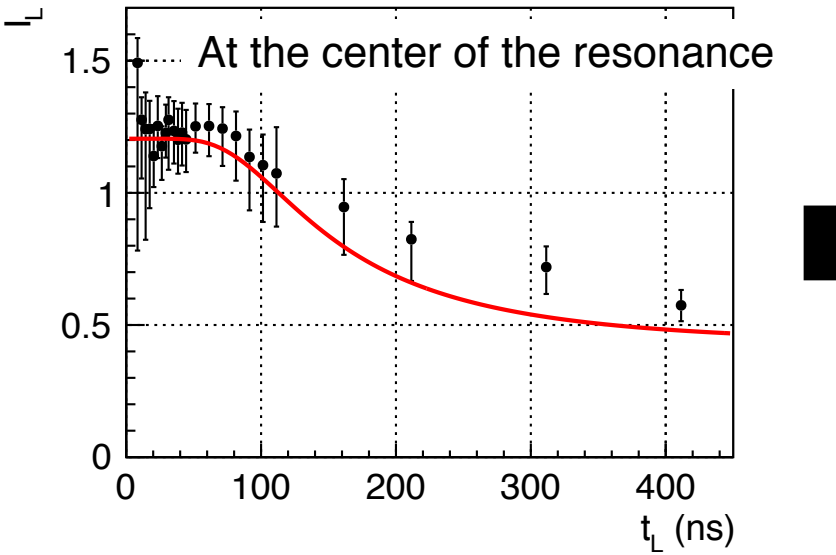

Laser timing

By optical Bloch eq.

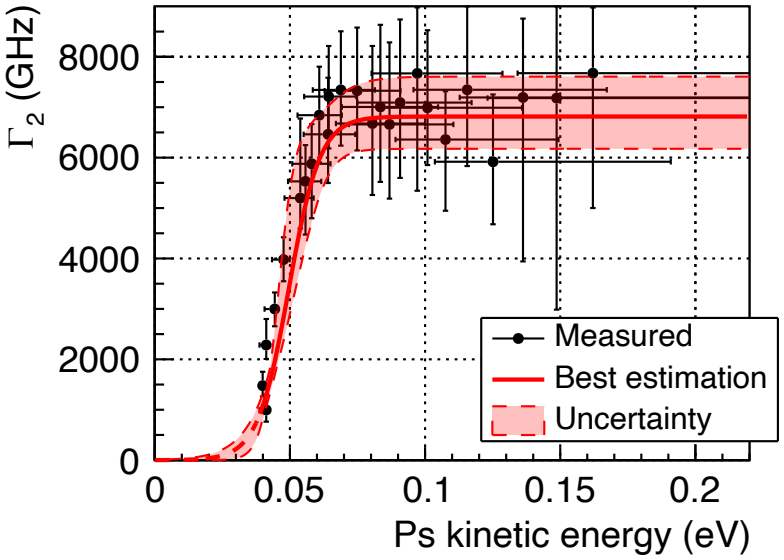

- Because Ps gradually slow down to aerogel temperature, energy dependence can be measured
- Enhanced decay rate in several THz varied with Ps kinetic energy

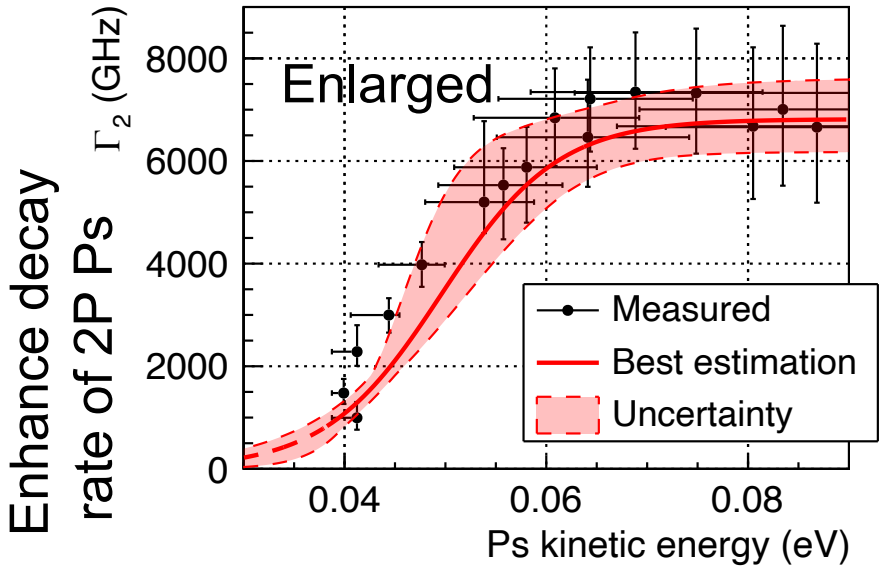

Decay rate was in the order of the classical collision rate

- Collision rate was estimated by kinetic energy and pore size
- Enhancement at 0.06 - 0.07 eV

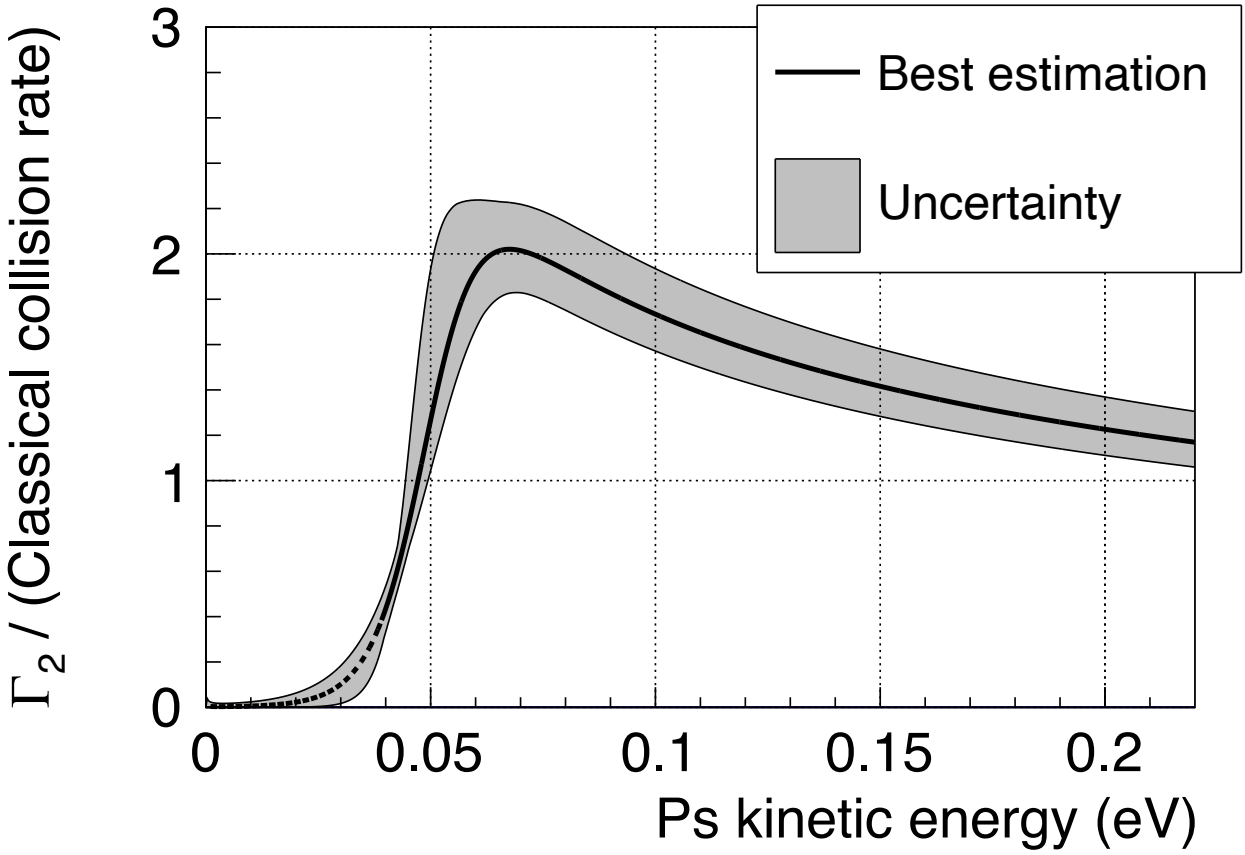

Small binding energy for n=2 can lead large decay probability

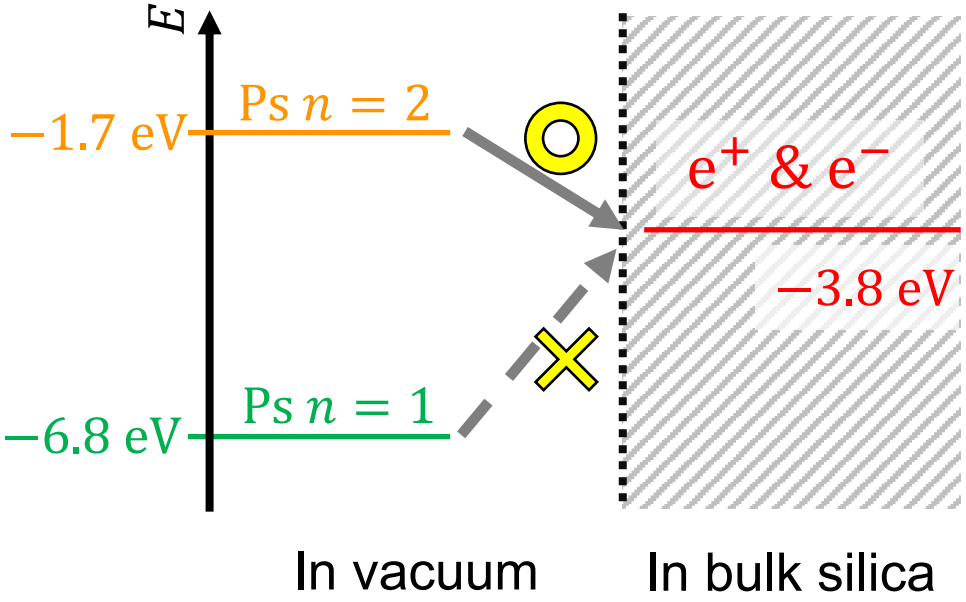

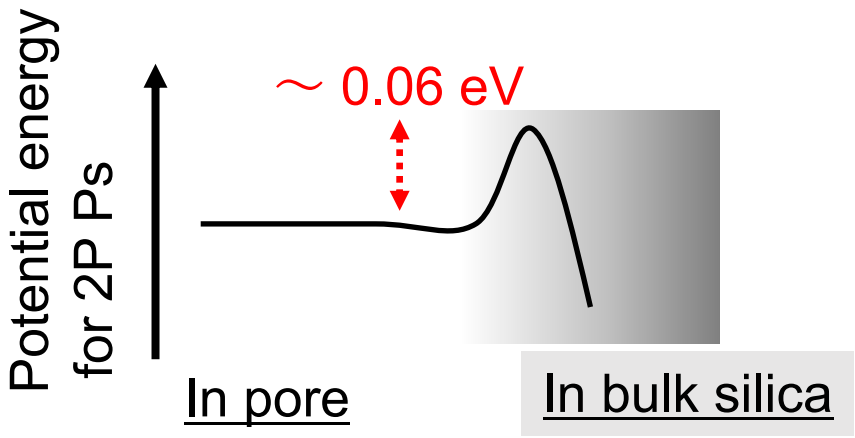

For silica, Ps in n=2 would not be more stable than dissociated state in the bulk

This would explain almost unity decay probability of 2P Ps

Energy dependence would have information on surface potential

More theoretical / experimental studies to test these models are necessary

Summary

- Unexplained results for interaction between 2P Ps and materials were found. We conducted basic studies.
- Understanding them will lead to new way to use Ps as a material probe, and breakthrough on Ps cooling for fundamental physics study

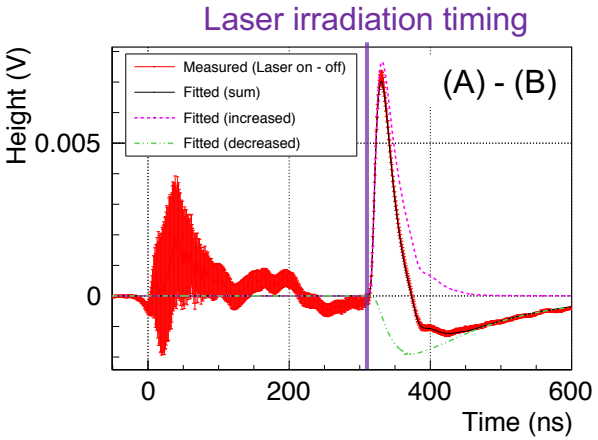

Difference by laser irradiation fitted by the following model

Enhanced decay was observed even in aerogel, which had less contaminants

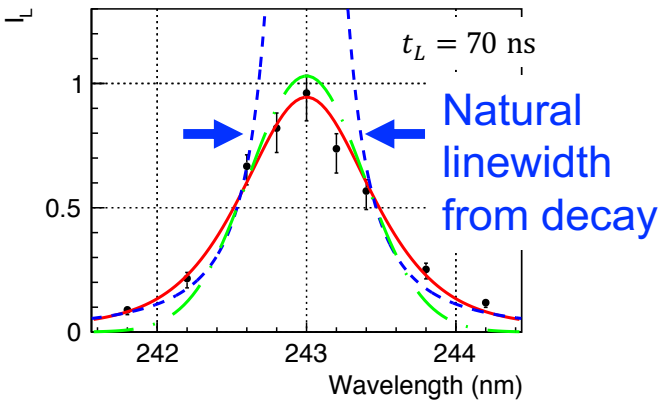

Inhomogeneous broadening

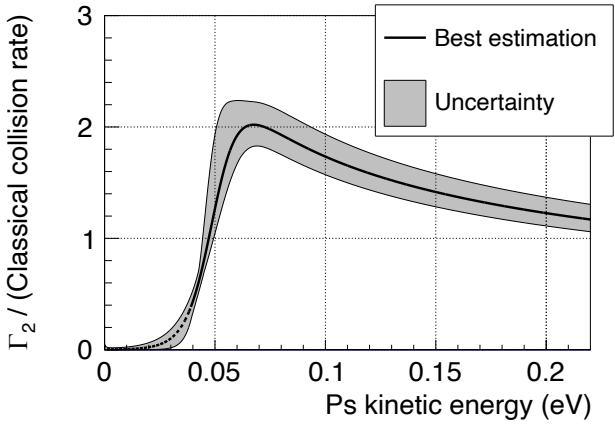

Very efficient dissociation

Backups

We used a silica aerogel

Porous silica sample as a positron-to-Ps converter
Also for Ps trapping

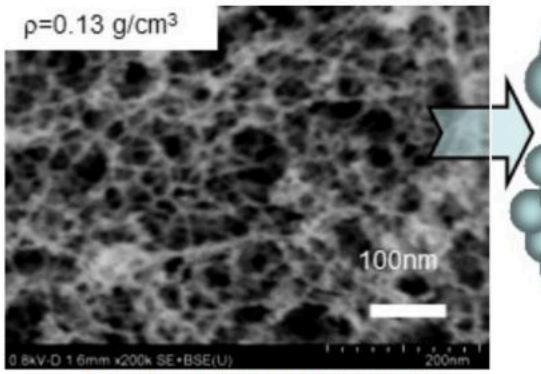

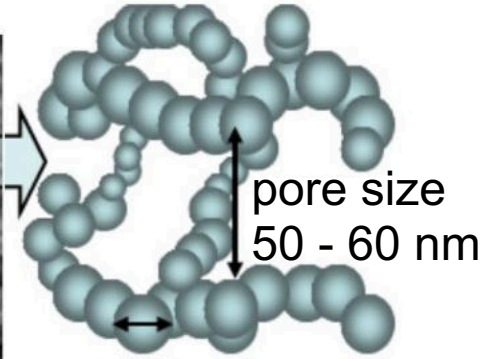

grain size
2 - 3 nm

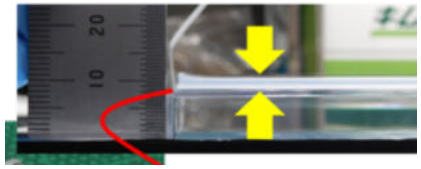

t = 0.5 mm

Silica aerogel
(from Japan Fine Ceramic Center)

Good points

- High Ps productivity by its high porosity
- High transparency for UV laser

1S Ps's Lifetime agreed with RTE Contaminants are much fewer

We measured Ps lifetime using Na-22

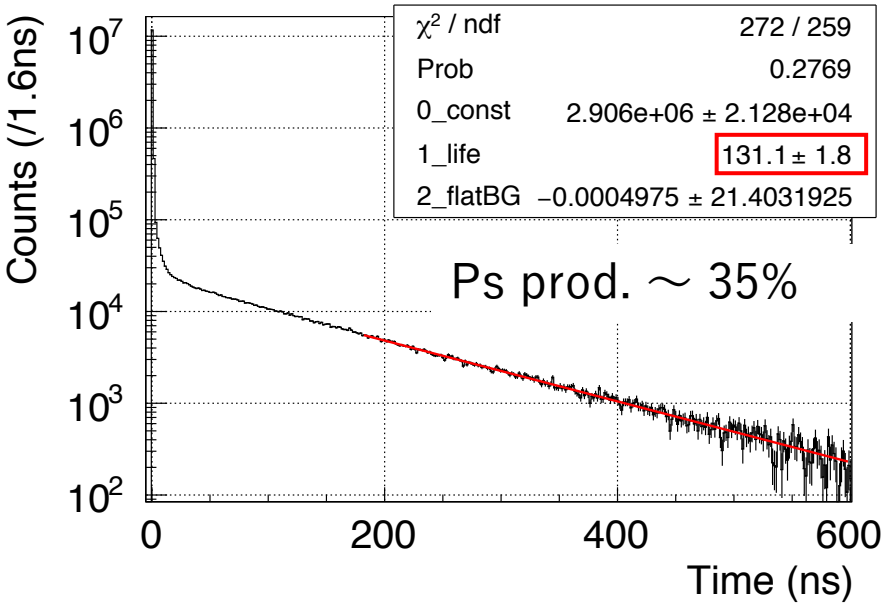

Bulk PALS measurement

In our aerogel :
D = 50 nm, τ ~ 130 ns

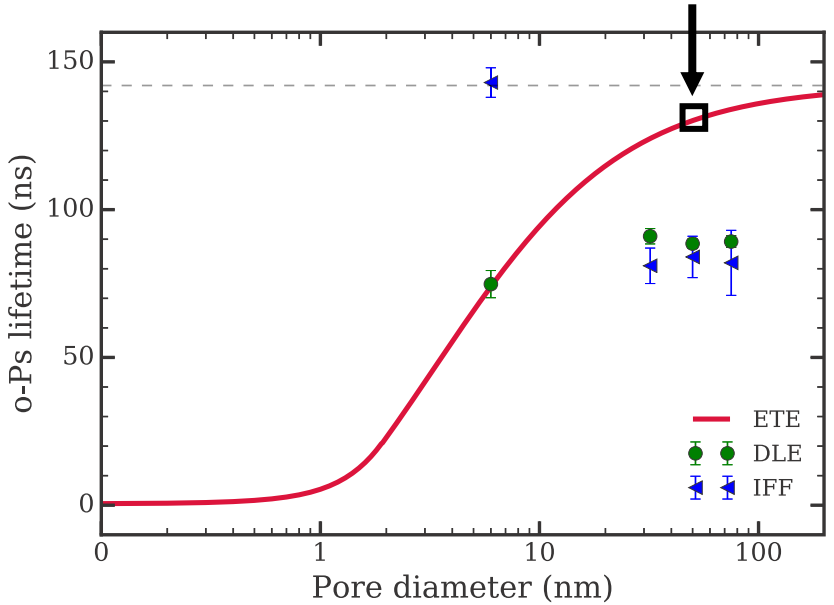

Cooper *et al.*, Phys. Rev. B **97**, 205302 (2018)

- Lifetime of 1S o-Ps was much longer than the previous work
- Contaminants are expected to be much fewer
  - ➢ We can test the hypothesis

高い崩壊率と広い線幅を引き起こす機構は謎
束縛したPsを励起するのは新しいテーマ

2011年 開いた空孔中 d = 5 nm
ディッケ束縛・2P崩壊しない・シフト

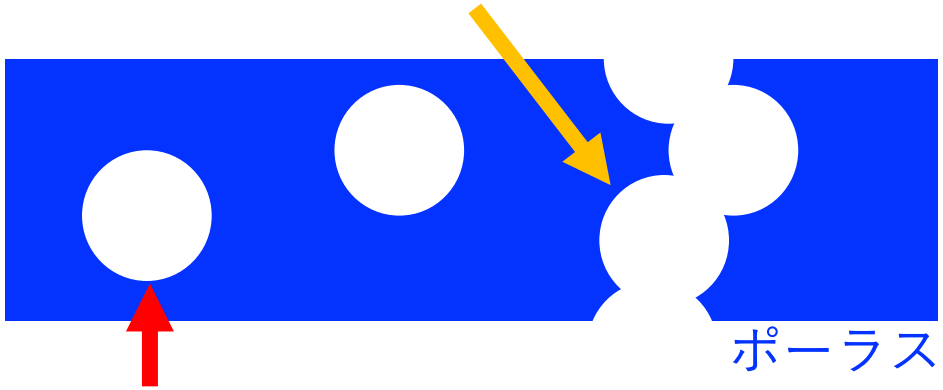

ポーラス
シリカ膜

先程の 2018年
閉じた空孔 d = 5 – 75 nm
広い線幅・2Pすぐ崩壊

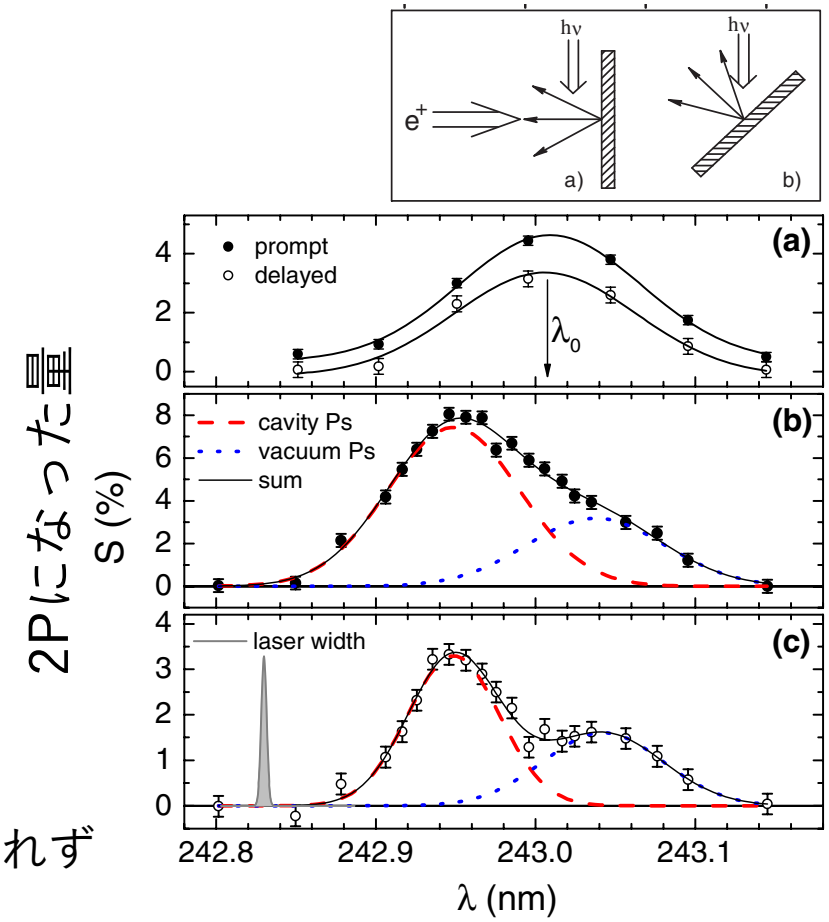

FIG. 2 (color online). Lineshapes measured for Ps

D. B. Cassidy et al. Phys. Rev. Lett. 106, 023401 (2011)

<u>2011年に行われた実験</u>
開いた空孔中では高い崩壊率と広い線幅がみられず

つい3週間前 MgO 中での結果が
同じグループから発表
2011年と同様の結果
L. Gurung et al. Phys. Rev. A 101, 012701 (2020)

低速陽電子ビームを使って Ps閉じ込めを確認

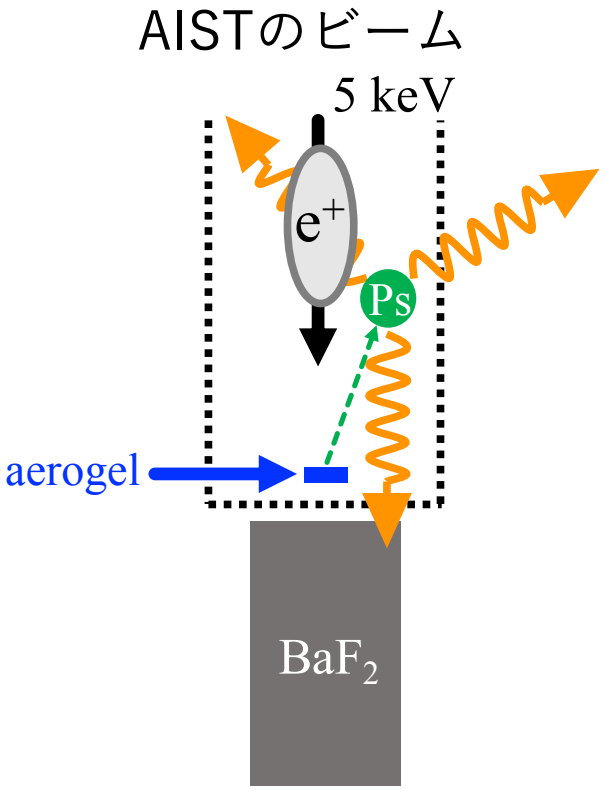

Psが飛び出て遠ざかると、
ガンマ線がとれなくなる
➢ 寿命が短くみえる

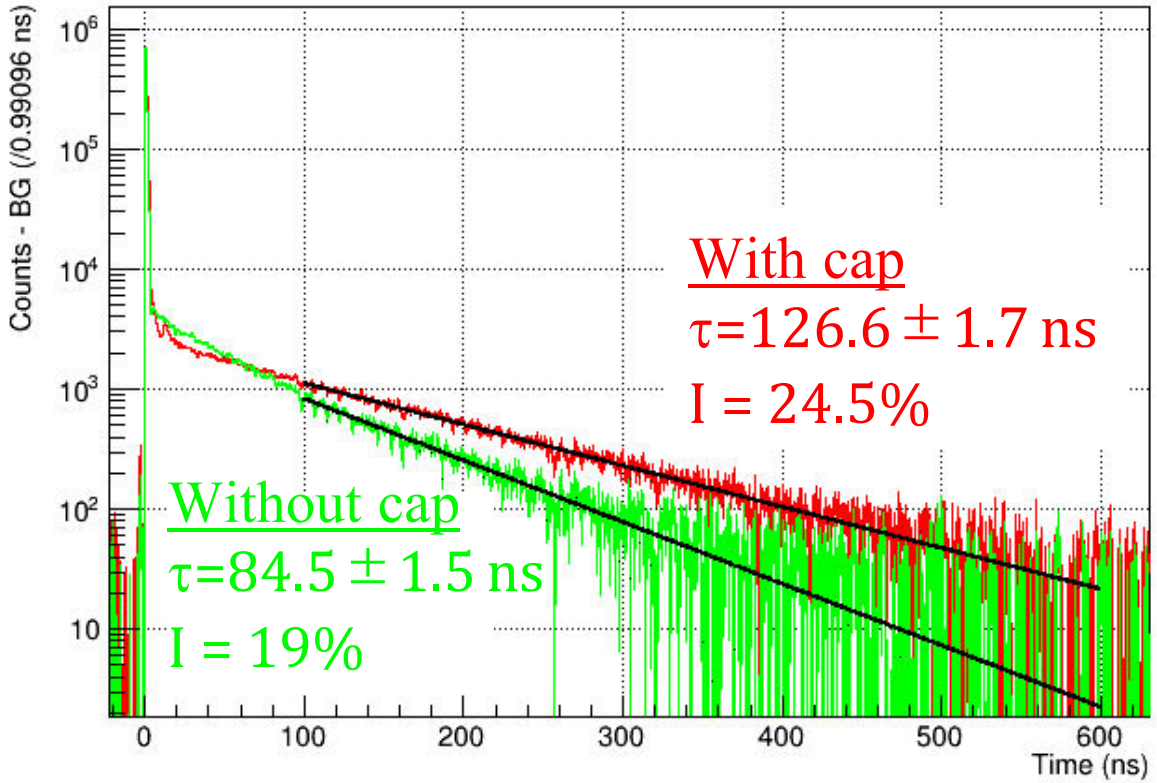

得られたタイミングスペクトル

非多孔質シリカのキャップで
寿命がNa-22での測定値に戻る

シリカエアロゲルが Ps Lyman-α の 243 nm に 吸収ピークをもたないことを確認

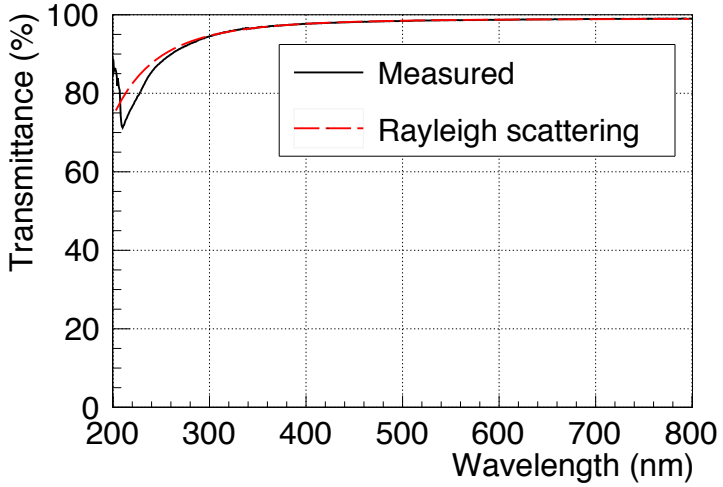

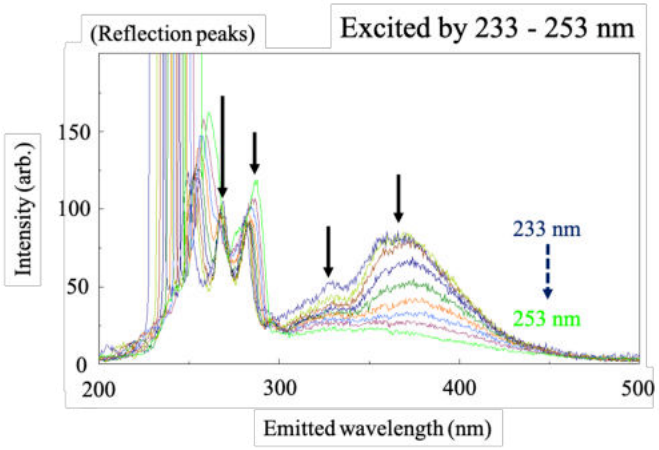

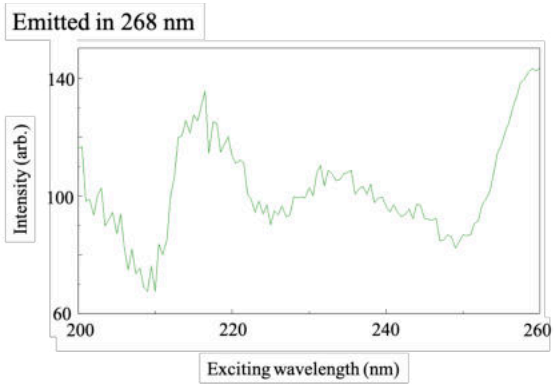

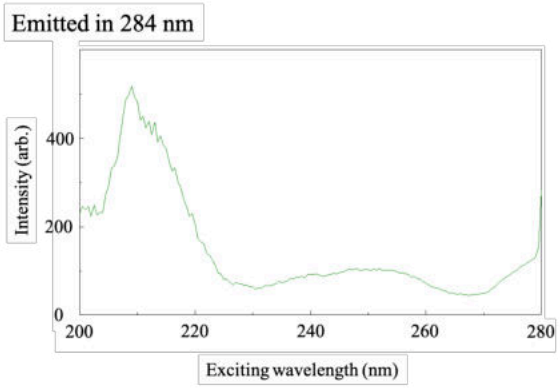

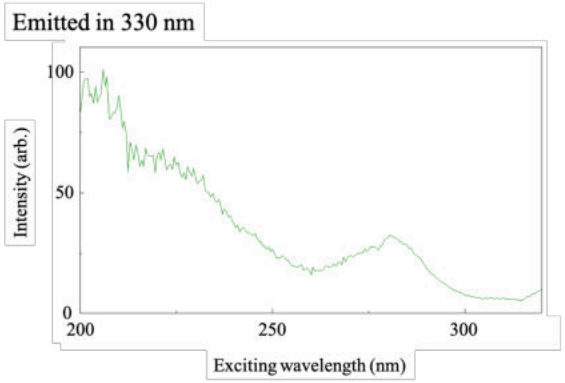

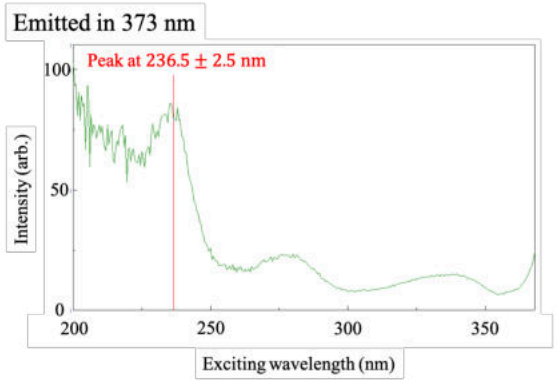

分光光度計、分光蛍光光度計で測定
共鳴により Lyman-α 遷移と分離可能

紫外OPOレーザーが必要な スペックを持つことを実測して確認

Table 2.4: Measured specification of the OPO laser.

Pulse energy	1 mJ
Pulse time duration	2 ns–5 ns
Line width (FWHM)	0.021 nm, 1.1×10^2 GHz
Beam diameter	6 mm
Repetition	10 Hz

← Lyman-αが十分飽和する

← 良い時間分解能

← 狭い線幅
（室温のドップラー幅の1/4）

↑ レーザー照射なしのデータを 40 Hz で同時に取得
（50 Hz（陽電子） − 10 Hz（レーザー））

解析方法1：SSPALS法
バンチで平均した波形にフィットする

バンチごとのPMT出力波形を平均し、モデル関数をフィットする

良：パイルアップをほどく必要がない｜**悪**：平均情報しか得られない

モデル関数：ガンマ線強度 ⊗ 陽電子バンチの時間波形 ⊗ 検出器の応答

求めたいパラメータを含む

例）

$$S(t) = \varepsilon_2 N_{\mathrm{prompt}} \delta(t)$$
$$+\left(\varepsilon_2 \Gamma_{po} + \varepsilon_3 \Gamma_s\right) N_{oPs} \exp\left(-\int_0^t \left(\Gamma'_{po}(t') + \Gamma_s\right) \mathrm{d}t'\right)$$

陽電子がPsを作らず
早く崩壊（prompt崩壊）
するカプトンで
得られる波形を再現

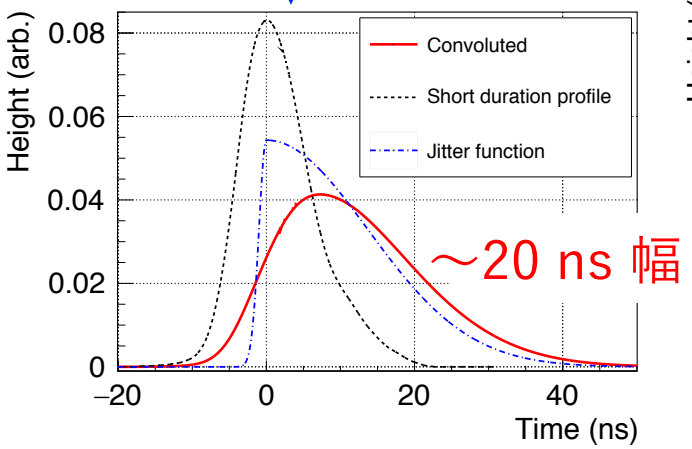

Na-22からの
ガンマ線を1つ
検出した波形

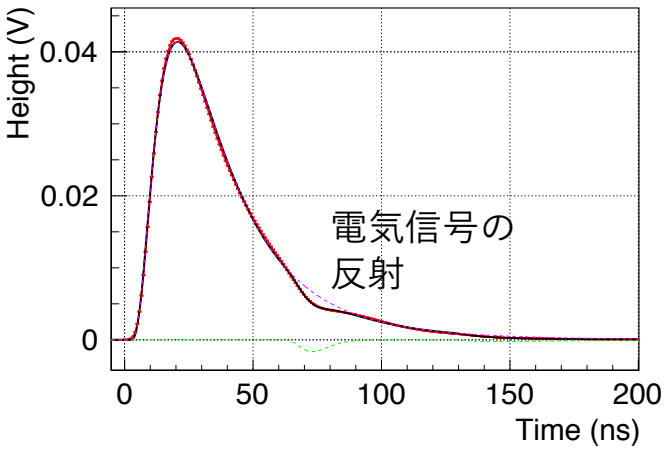

解析方法2：Pulse-by-pulse法
ガンマ線検出したパルスを1つずつ解析する

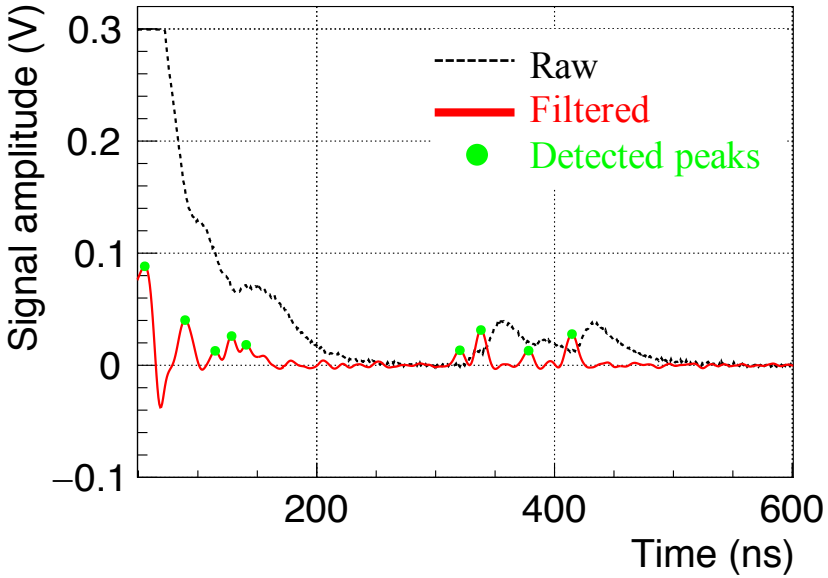

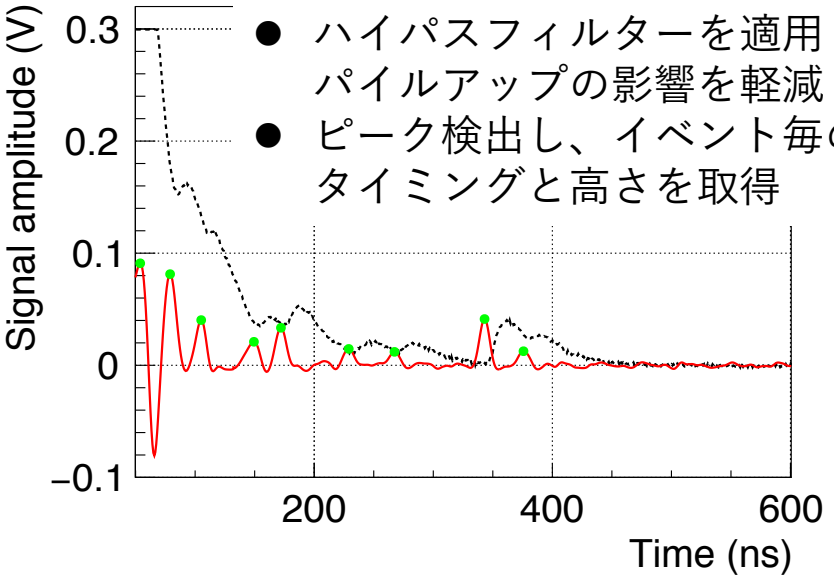

- ハイパスフィルターを適用してパイルアップの影響を軽減
- ピーク検出し、イベント毎のタイミングと高さを取得

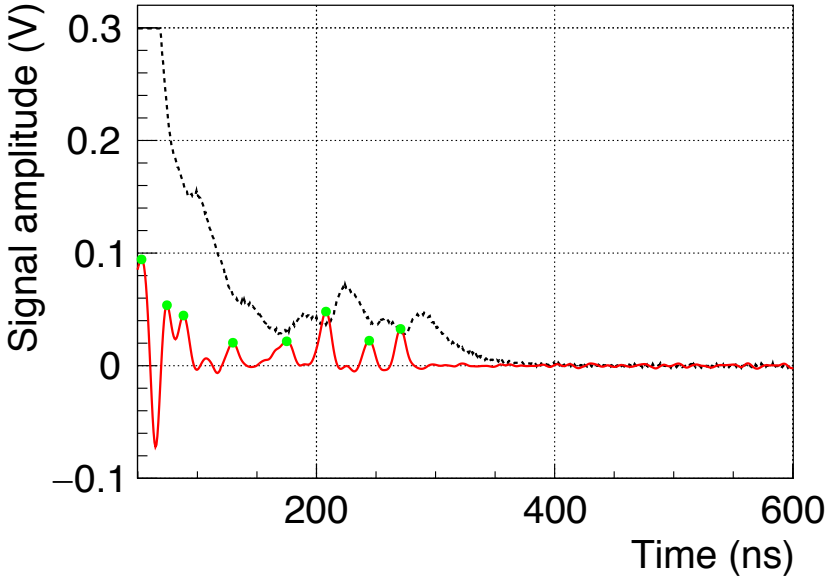

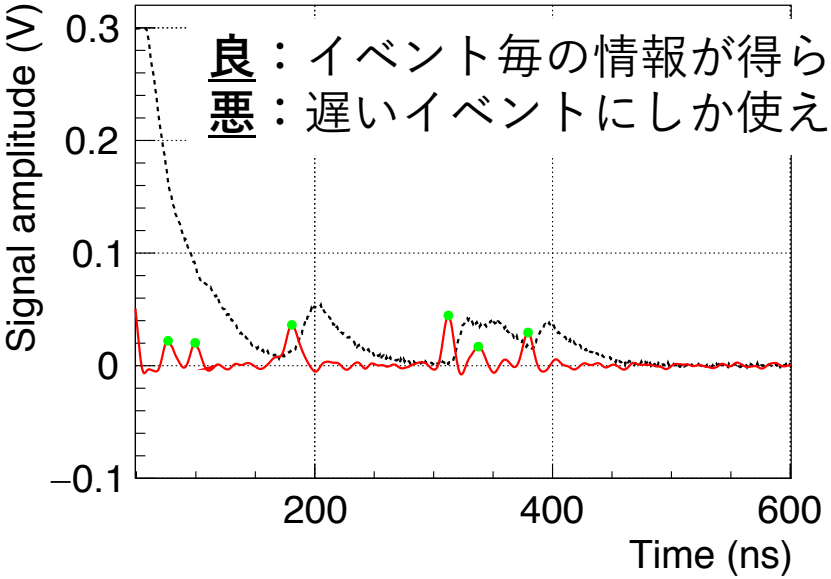

良：イベント毎の情報が得られる
悪：遅いイベントにしか使えない

Pulse-by-pulseで寿命が正しく求まる

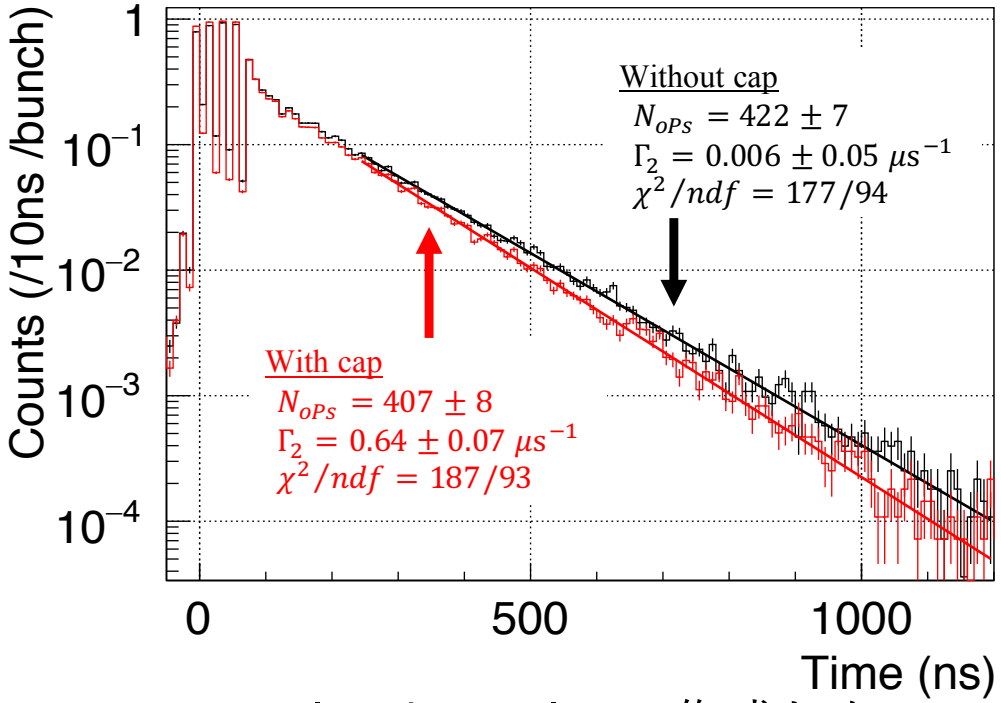

Pulse-by-pulseで作成した
タイミングスペクトル

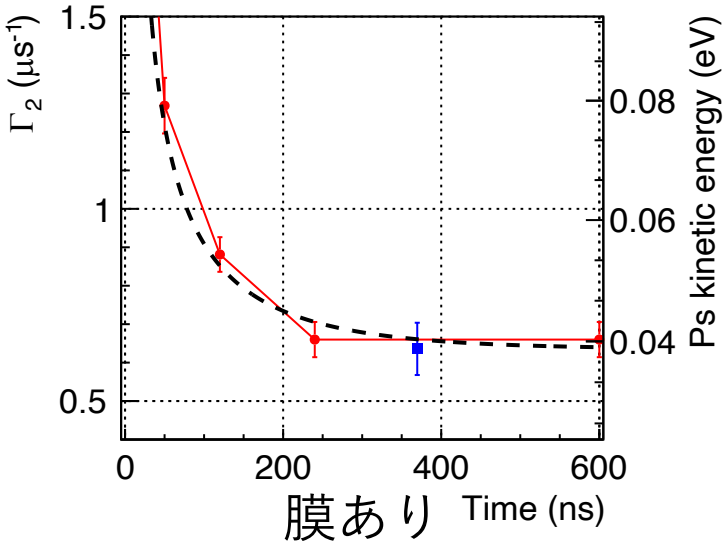

膜あり

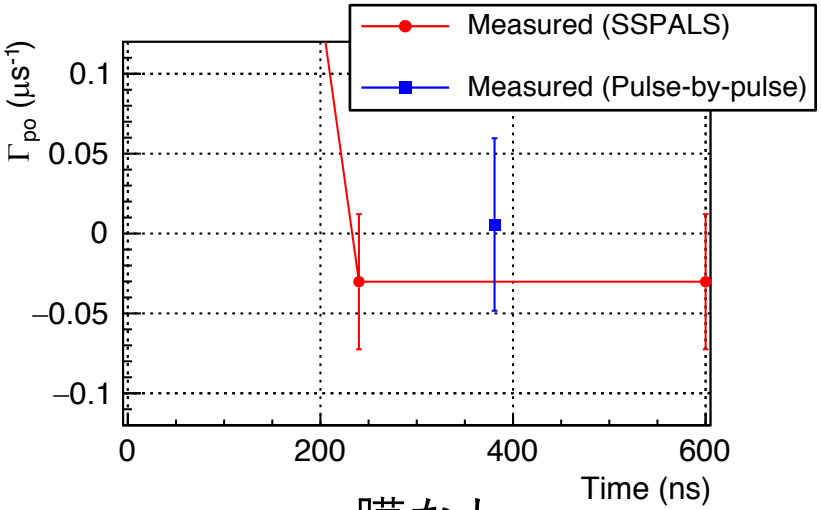

膜なし

- 信号のタイミングスペクトルが得られる
- 他の手法と一致する

Pulse-by-pulse で エネルギースペクトルが得られる

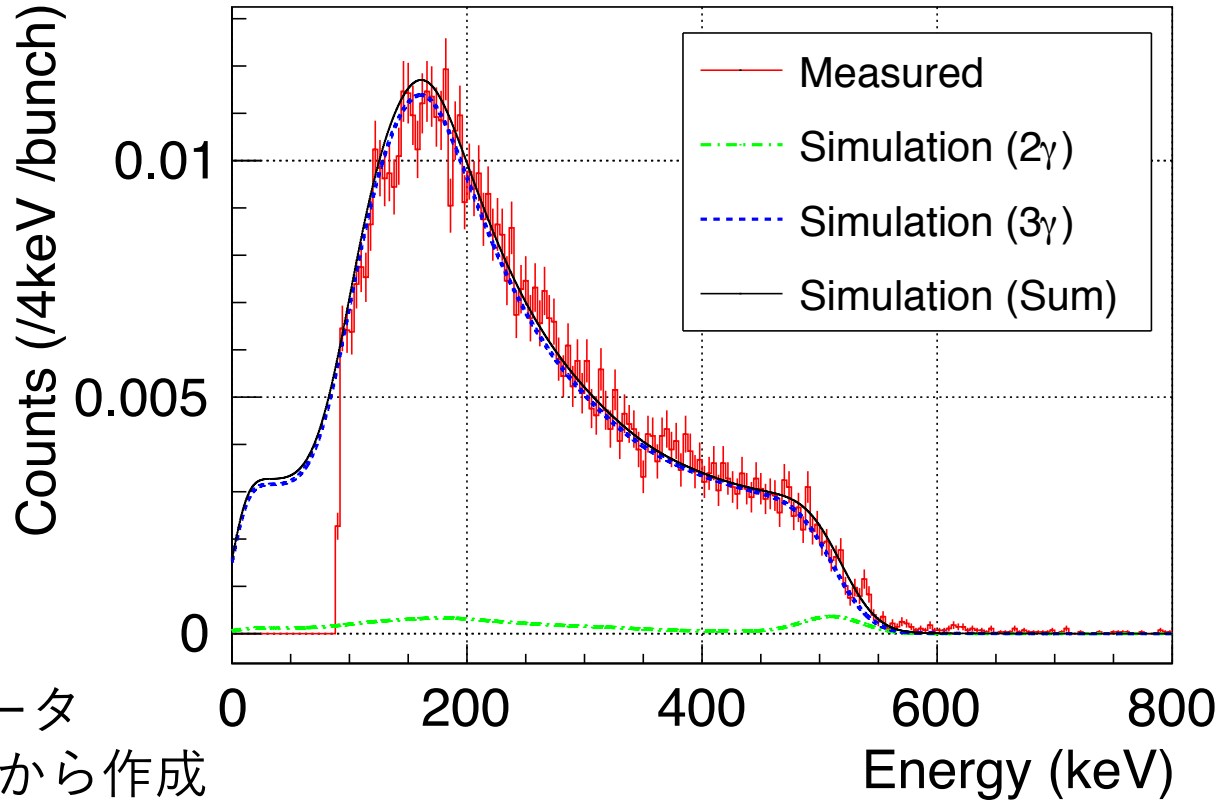

Pulse-by-pulseで作成した
エネルギースペクトル

- 膜ありエアロゲルのデータ
- 400 ns 以降のイベントから作成
- Geant4 MC シミュレーションと比較してよく合っている
  分布の平均値で2%の精度
  （系統不確かさ）

真空中でPsを励起し系が設計通りに動いているか確認

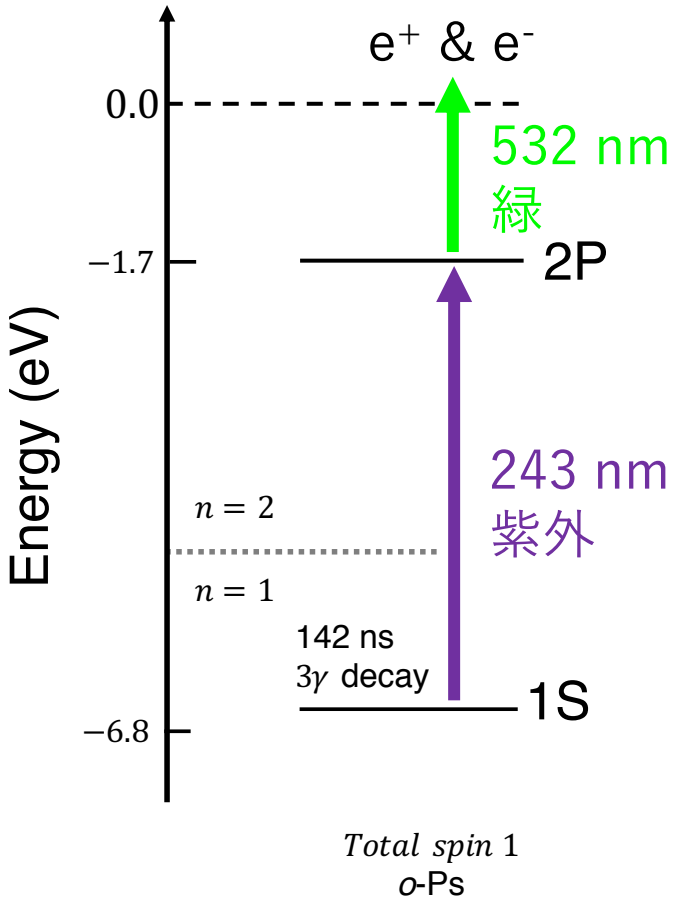

- エアロゲルの空孔外、真空中で2P状態にし、狙ったとおりに Lyman-α 遷移を誘導できるか確認
- 532 nm の緑パルスレーザーを同時に入射し、2P状態のみを電離する
- 電離陽電子の対消滅がシグナル

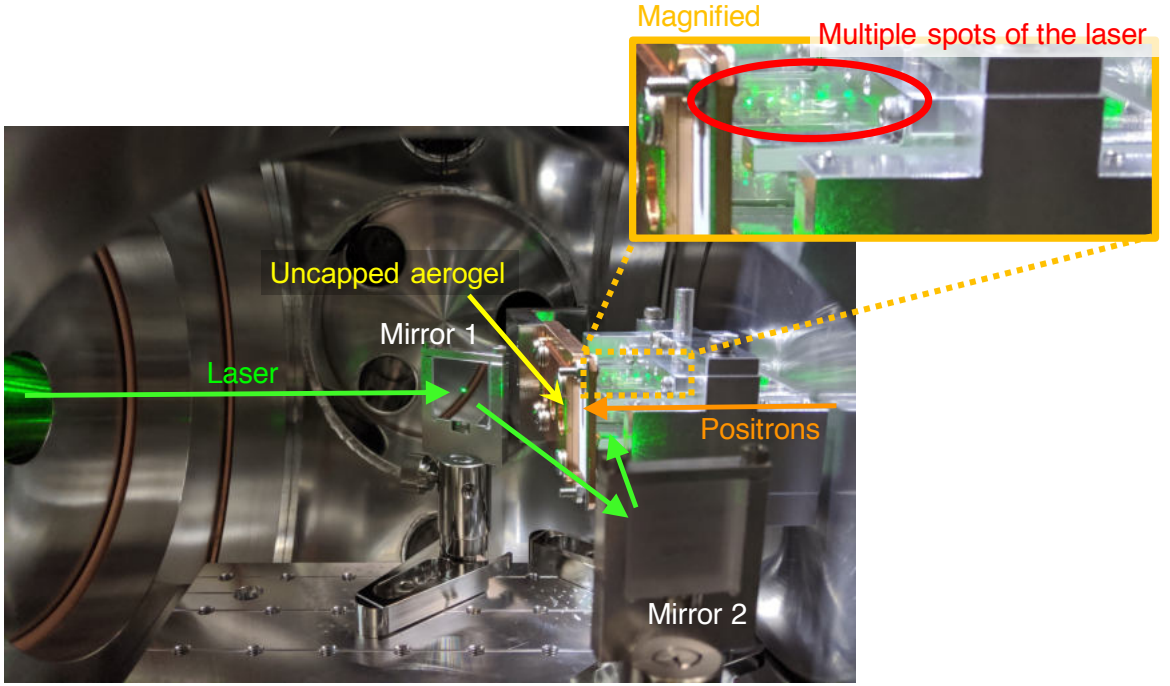

真空中で2Pに励起できる
真空中では2P-Psはガンマ線に崩壊しない

■：紫外レーザーだけでは
電離陽電子が生じない

●：紫外 & 緑レーザーを
同時入射すると243 nm が
中心の Lyman-α 共鳴曲線
がみられる

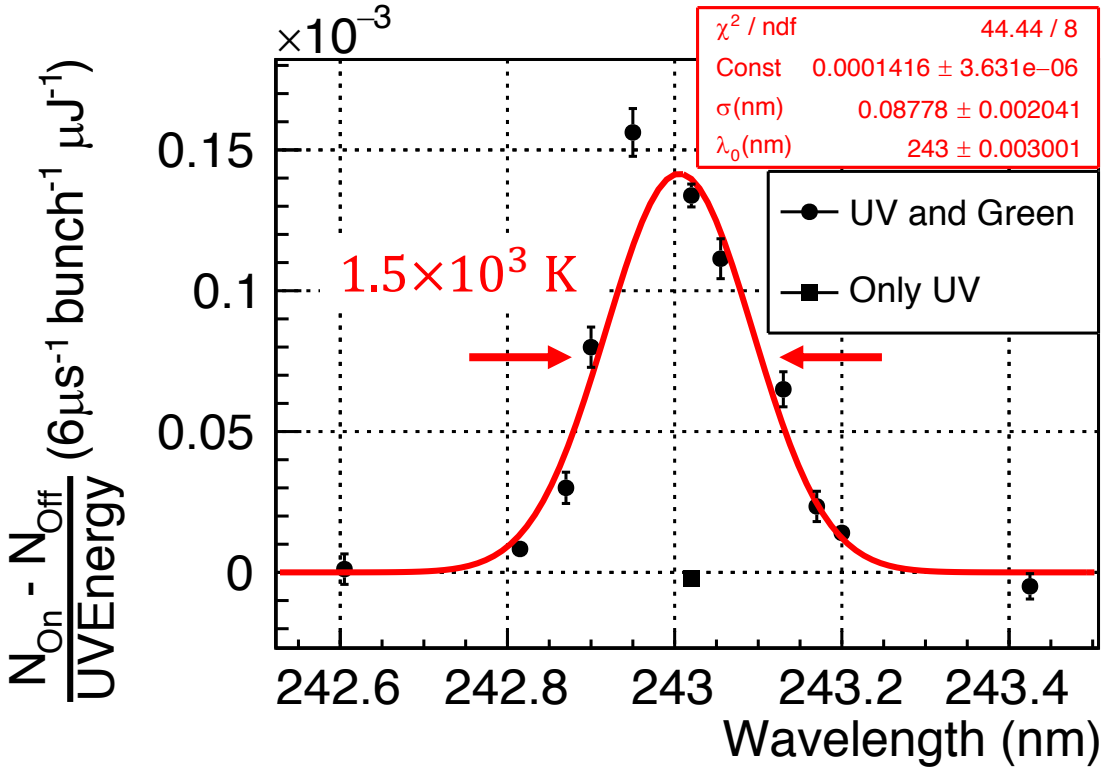

幅は Pick-off 崩壊率から
求まる平均運動エネルギー
（0.20 eV）から予想される
ドップラー幅

Pulse-by-pulse での タイミングスペクトルでも確認

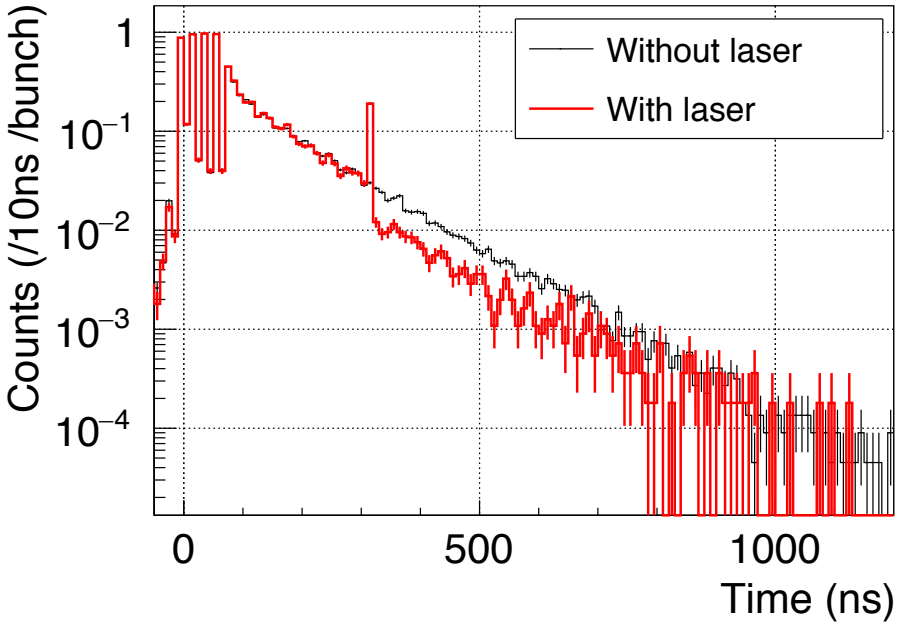

Pulse-by-pulse で作成した
タイミングスペクトル

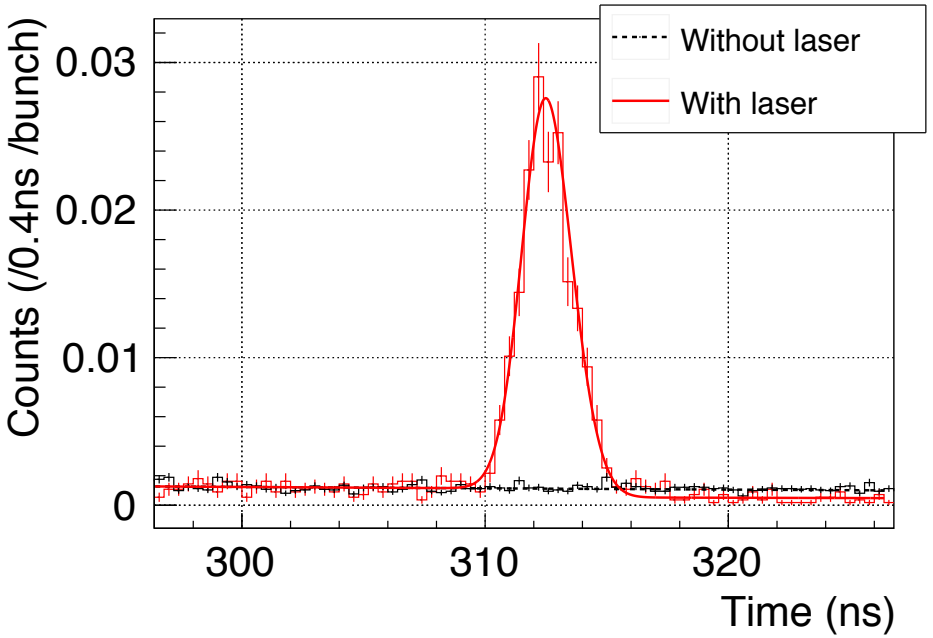

レーザー照射タイミングを
拡大

傾きが緩やかになっている = 寿命が延びている
のは速いPsが崩壊しやすいから（後述）

崩壊は243 nm（Ps Lyman-α）付近でのみ生じる 2P状態になって崩壊している

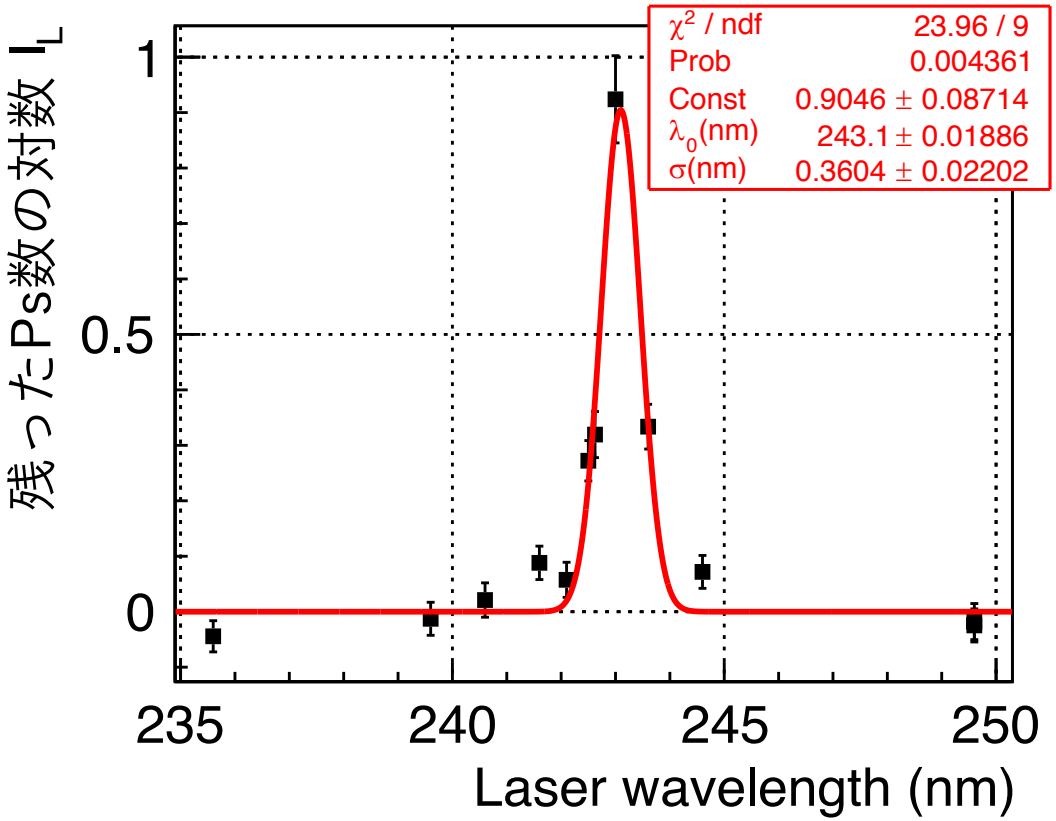

結論その1

- 1S-Psが束縛されないエアロゲルでも、2P状態はすぐガンマ線に崩壊する
- 2P状態特有の性質（小さい束縛エネルギーや大きい電気感受率）が崩壊の原因

誘導される崩壊率は
レーザーの強度・波長、 2P-Psの崩壊率に依存

ガンマ線強度の式

$$S(t) = \varepsilon_2 N_{prompt}\delta(t)$$

レーザー照射によるPsの崩壊率 Γ_L
2光子崩壊であることを
Pulse-by-pulse で確認した

$$+ (\varepsilon_2\Gamma_{po}(t) + \varepsilon_3\Gamma_s + \varepsilon_L\Gamma_L(t))N_{oPs}\exp\left(-\int_0^t (\Gamma_{po}(t') + \Gamma_s + \Gamma_L(t'))\mathrm{d}t'\right)$$

Γ_L はレーザーの強度、波長、Γ_2に依存する

仮定したレーザー場の時間波形包絡線と同じガウス型

$$\Gamma_L(t) = \frac{I_L}{\sqrt{2\pi}\sigma_L}\exp\left(-\frac{t-t_L}{2\sigma_L^2}\right)$$

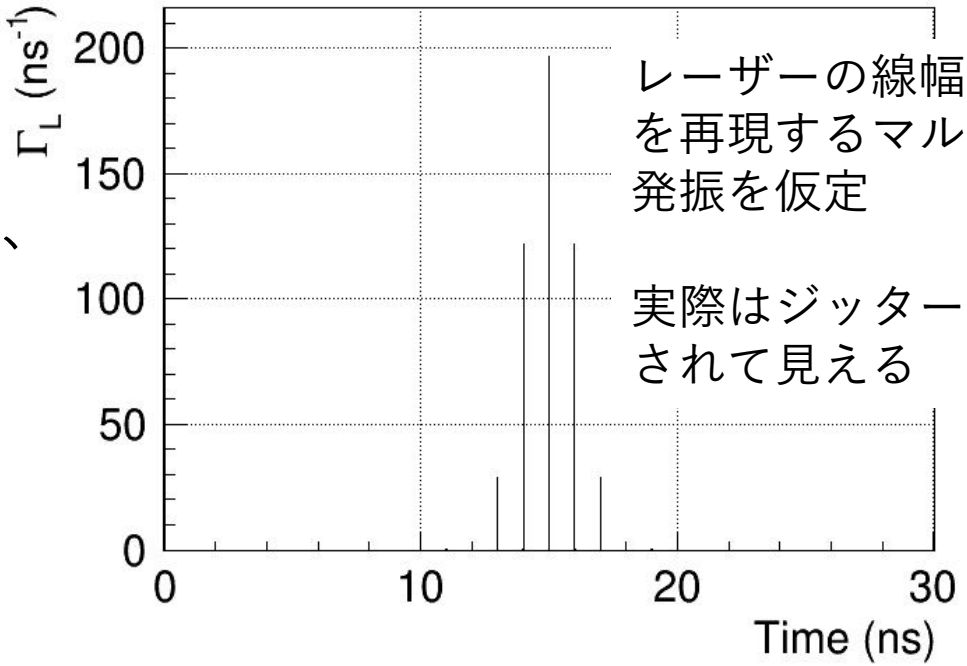

レーザーの線幅・時間幅を再現するマルチモード発振を仮定

実際はジッターでスメアされて見える

実測したレーザーのパラメータを入力して得られる典型的な計算例

共鳴曲線は自然幅で広がる

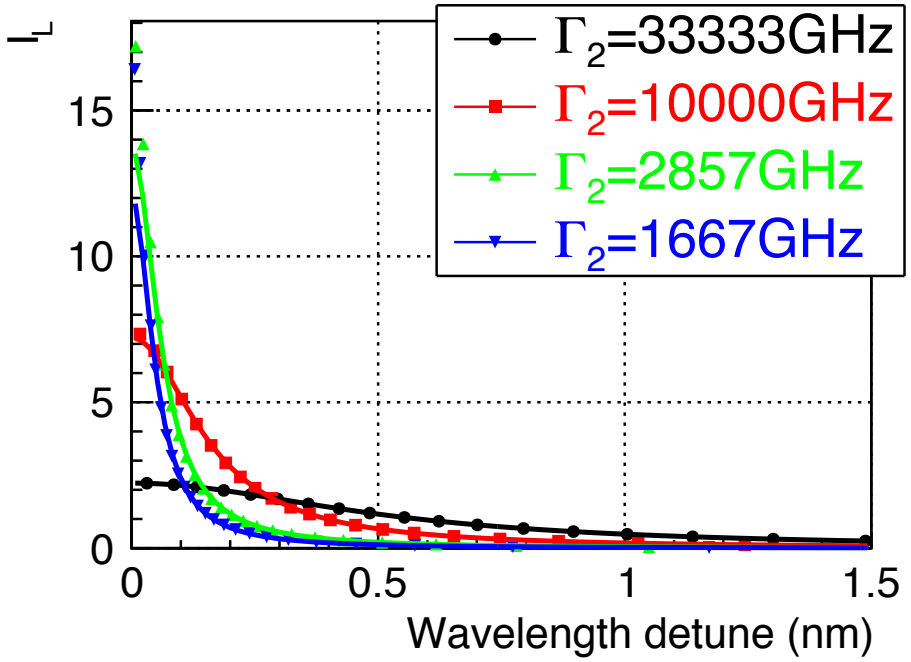

残った数の対数

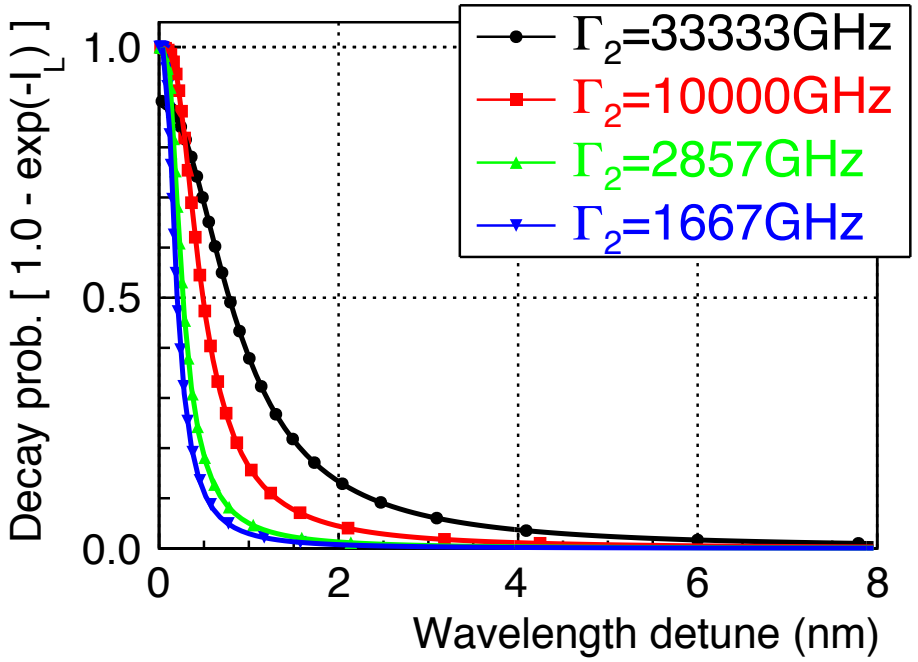

消滅するPsの割合

測定で得られる共鳴曲線を再現する
Γ_2を求める

データを説明できる

$I_L = 0.74 \pm 0.05$

$\exp(-I_L) = 52 \pm 3\%$

Pulse-by-pulse で得られる
タイミングスペクトル

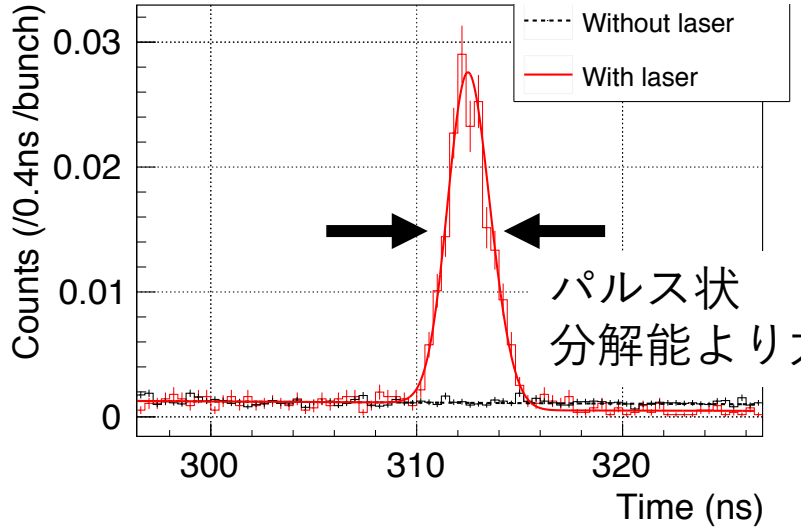

パルス状
分解能より太い

MCで求めた検出効率を使って
増えた量と減った量をコンシストに説明できる

2つの解析手法で結果が一致

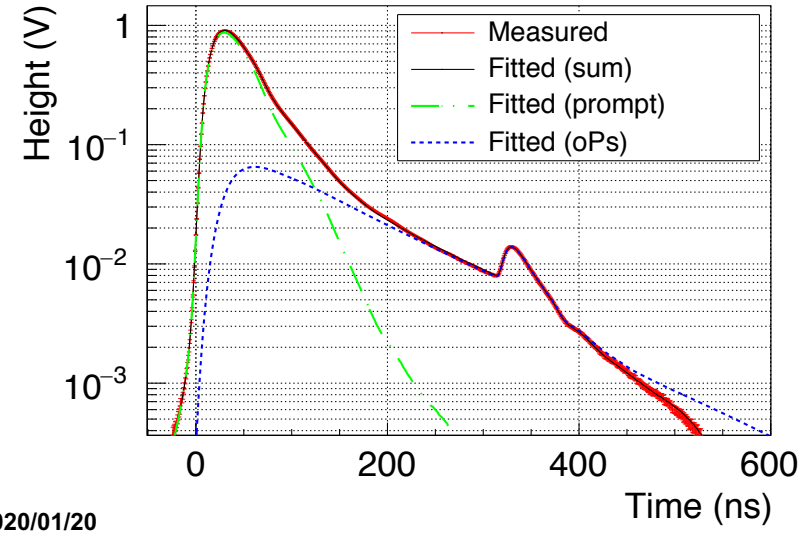

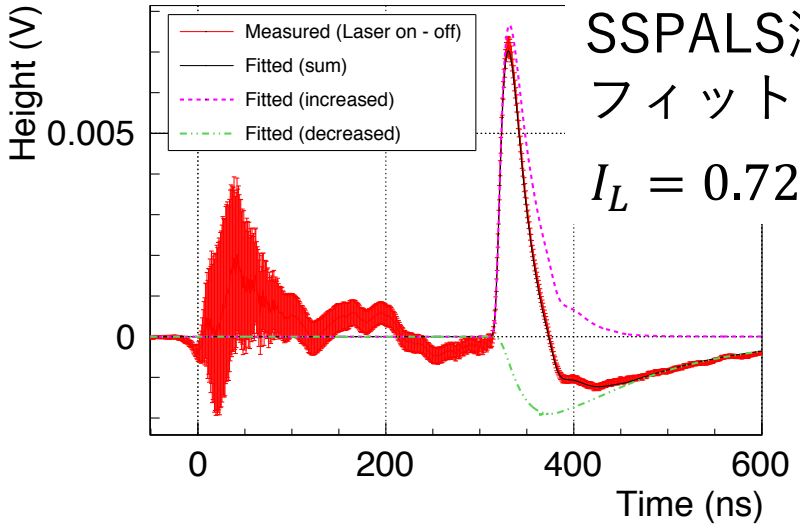

SSPALS法で
フィット

$I_L = 0.72 \pm 0.04$

レーザー波長・タイミングを変えて 共鳴曲線のPs運動エネルギー依存性を測る

- Psが熱化過程により徐々に運動エネルギーを失うため、レーザー照射タイミングを変えることで Γ_2 の運動エネルギー依存性測定
- 0.04 — 0.2 eV まで変化
- 測定したPick-off 崩壊率を含むよう不確かさを見積もった

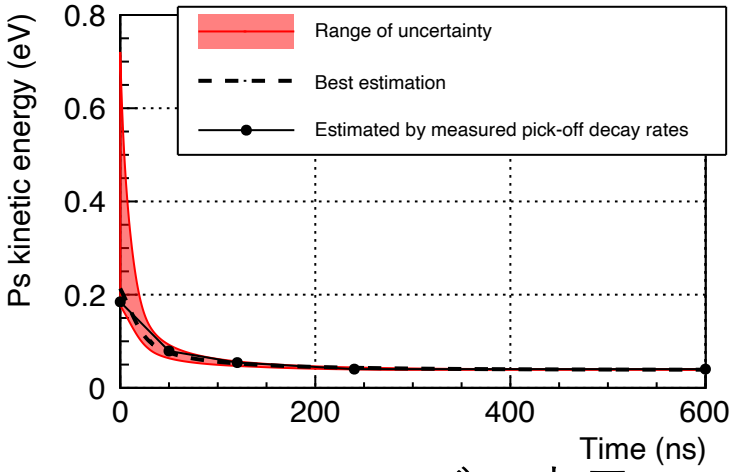

フルレンジで表示

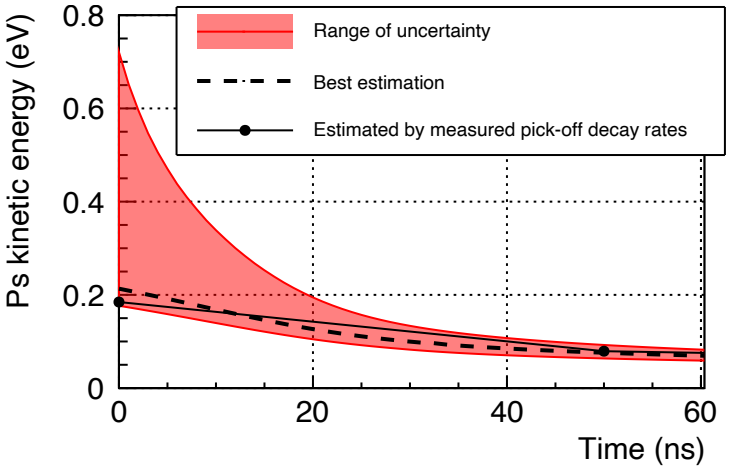

早いところ

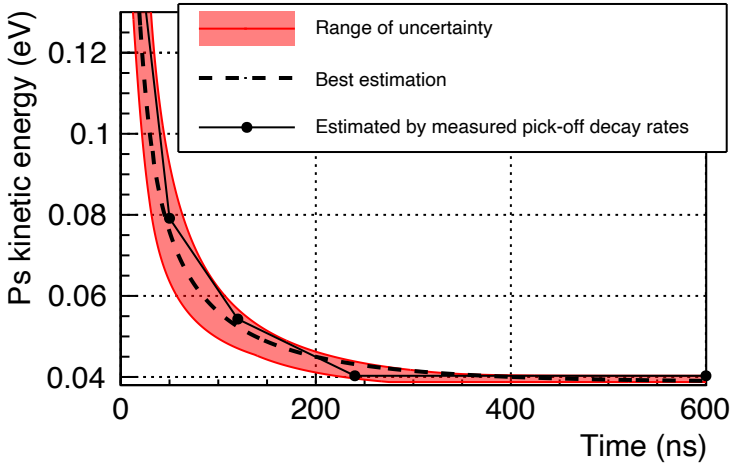

遅いところ

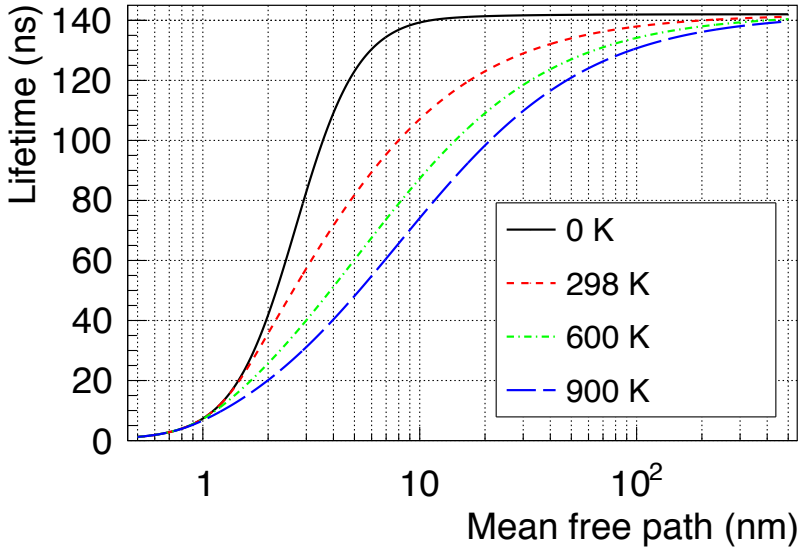

(a) In lifetimes.

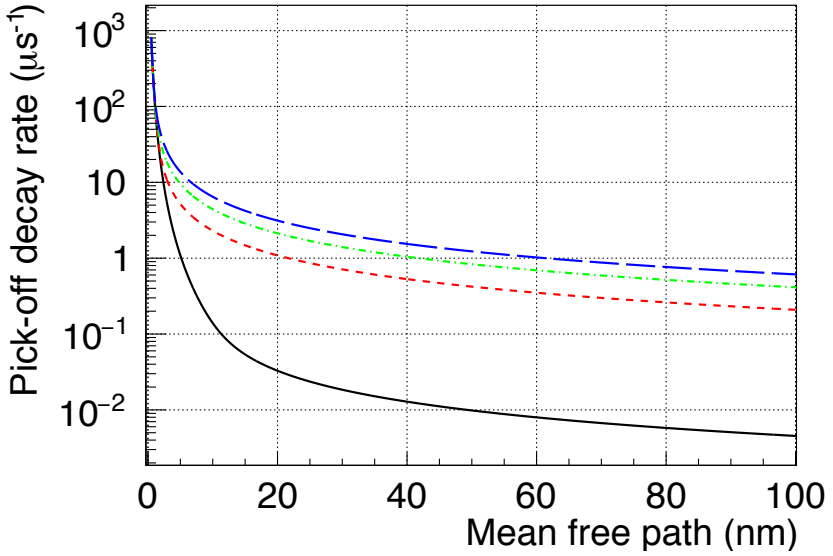

(b) In decay rates.

Figure 1.3: Dependence of the pick-off decay rate on mean free path for various temperatures of Ps.

$$\frac{dE}{dt} = -\frac{2}{LM}\sqrt{2m_{Ps}E}\left(E - \frac{3}{2}k_B T\right)$$

$$\frac{1}{M(E)} = \frac{C_1}{M_{Opt}(E)} + \frac{1}{M_0 + C_2/E}, \quad \text{Global fit}$$

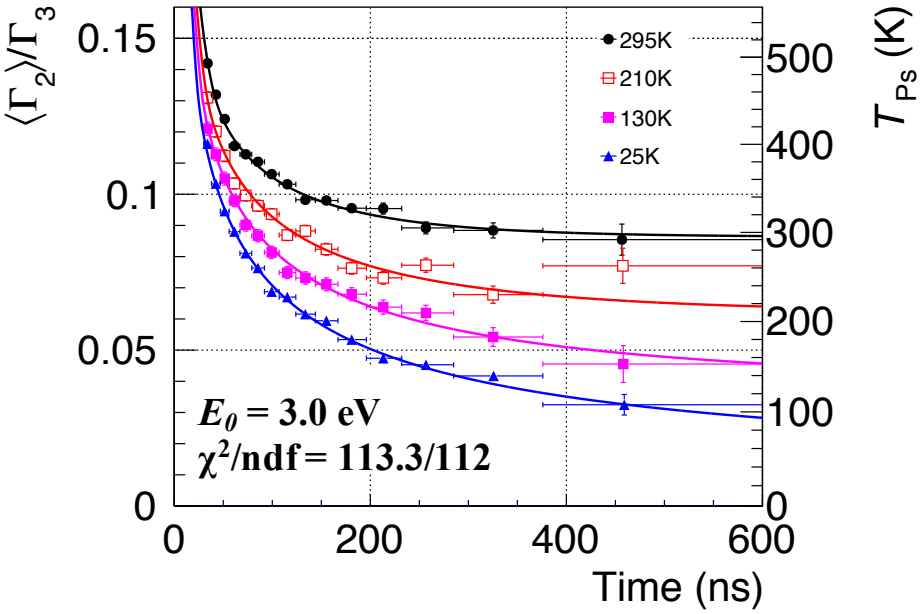

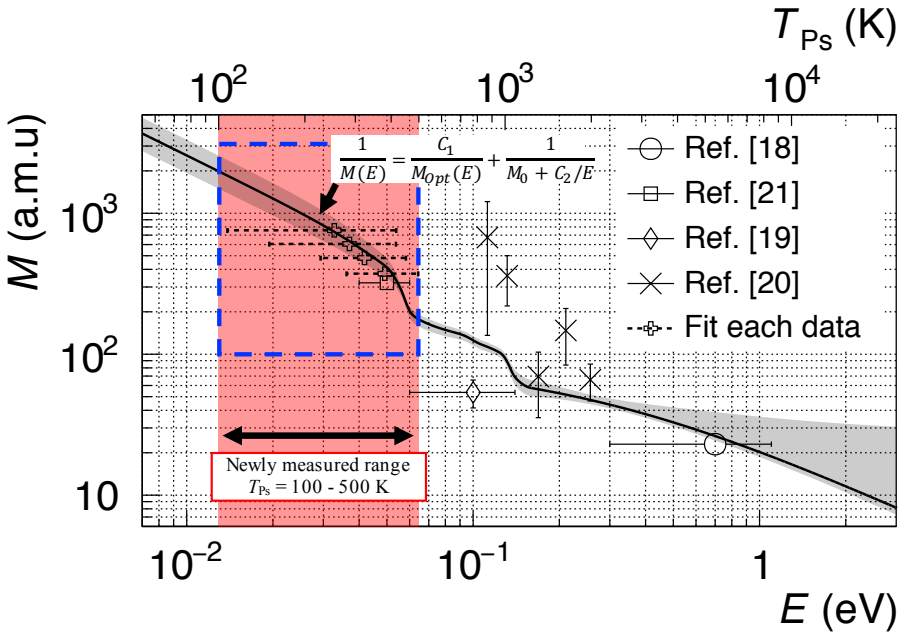

ファブリーペロー
ソリッドエタロン

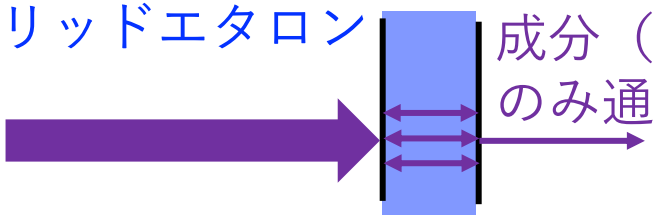

共鳴条件を満たした
成分（波長・横モード）
のみ通過する

Measured points

Etalon's sharp transmittance

Laser spectrum ⊛ Etalon transmittance

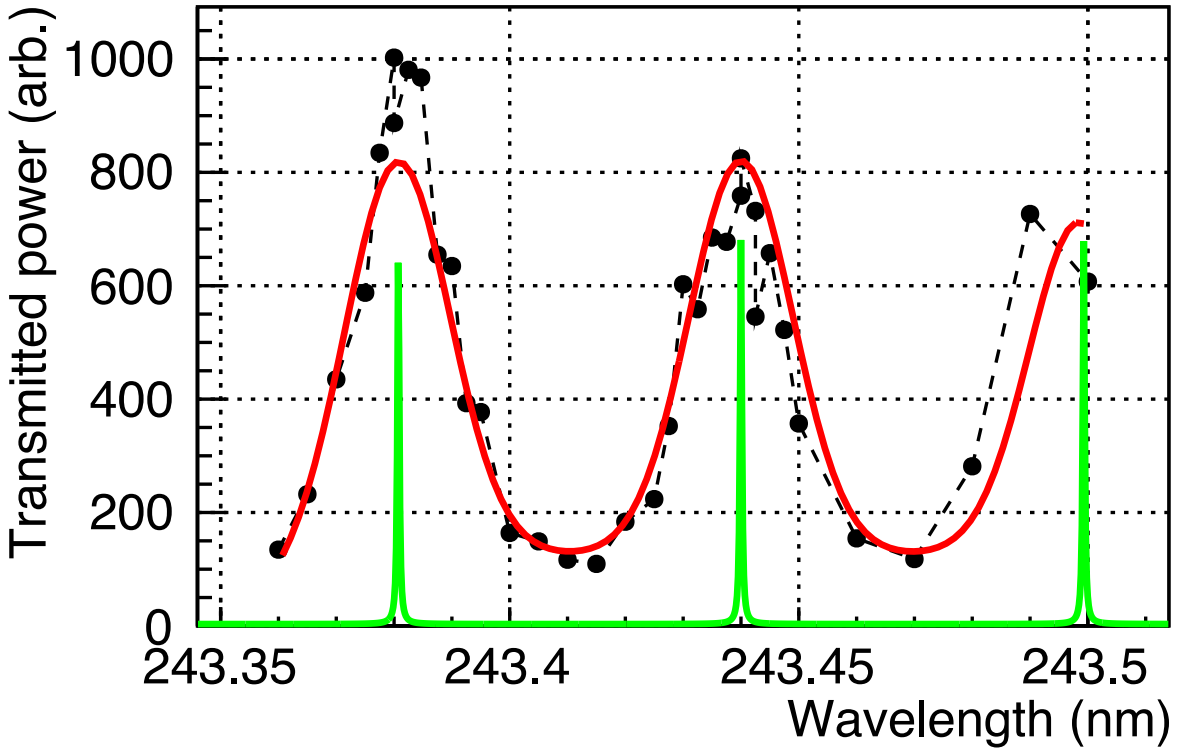

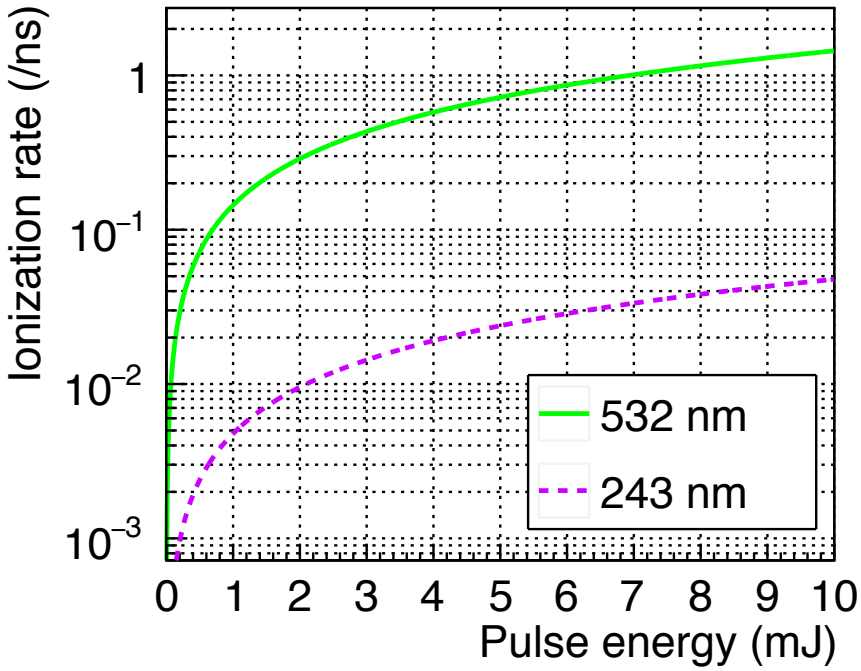
Ionization rate (/ns)
1
10^{-1}
10^{-2}
10^{-3}
0 1 2 3 4 5 6 7 8 9 10
Pulse energy (mJ)
532 nm
243 nm

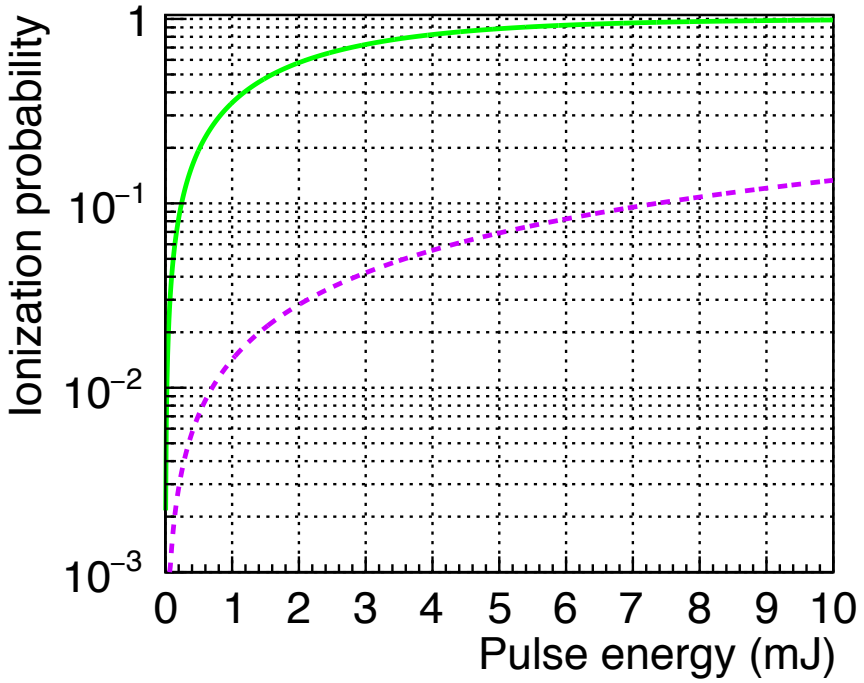
Ionization probability
1
10^{-1}
10^{-2}
10^{-3}
0 1 2 3 4 5 6 7 8 9 10
Pulse energy (mJ)

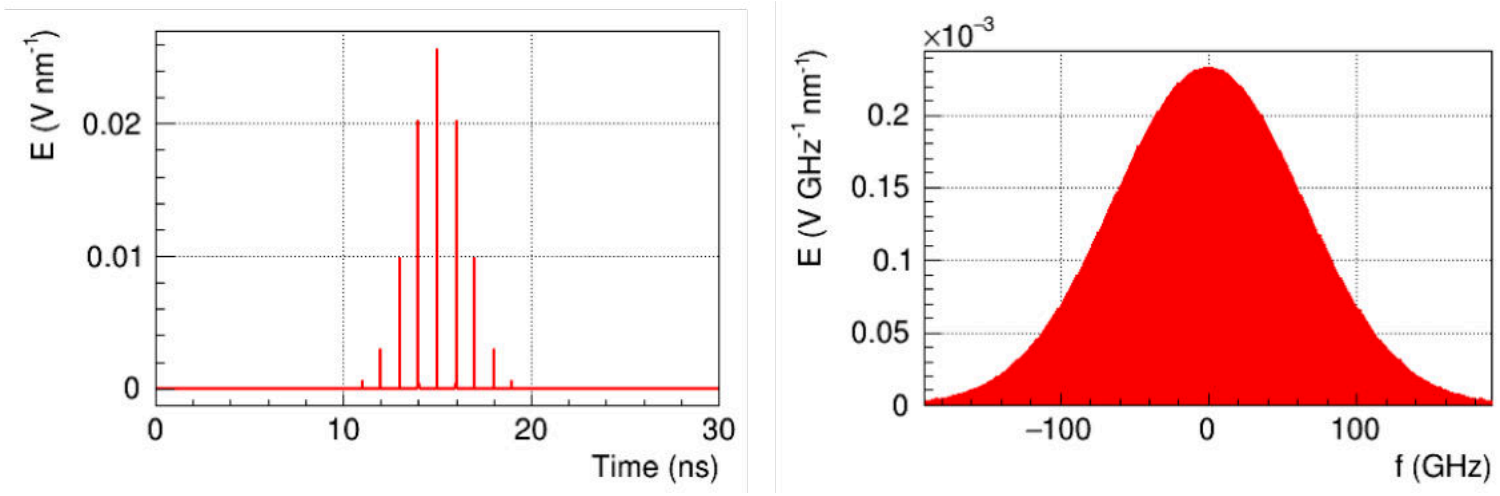

Figure 2.22: Simulated laser field. (Left) timing profile. (Right) Frequency spectrum. The power profile and spectrum can be obtained by squaring the field amplitudes to be compared with the measured pulse time duration and the band width.

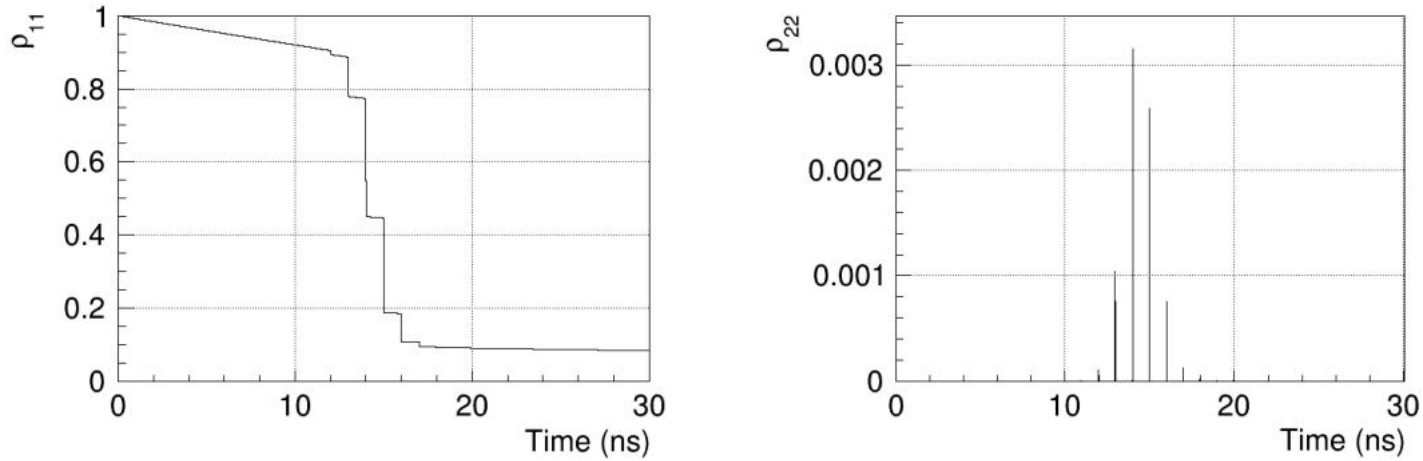

(a) ρ_{11} element.

(b) ρ_{22} element.

Figure 2.23: Example of density matrix by the model calculation of the Ps excitation.

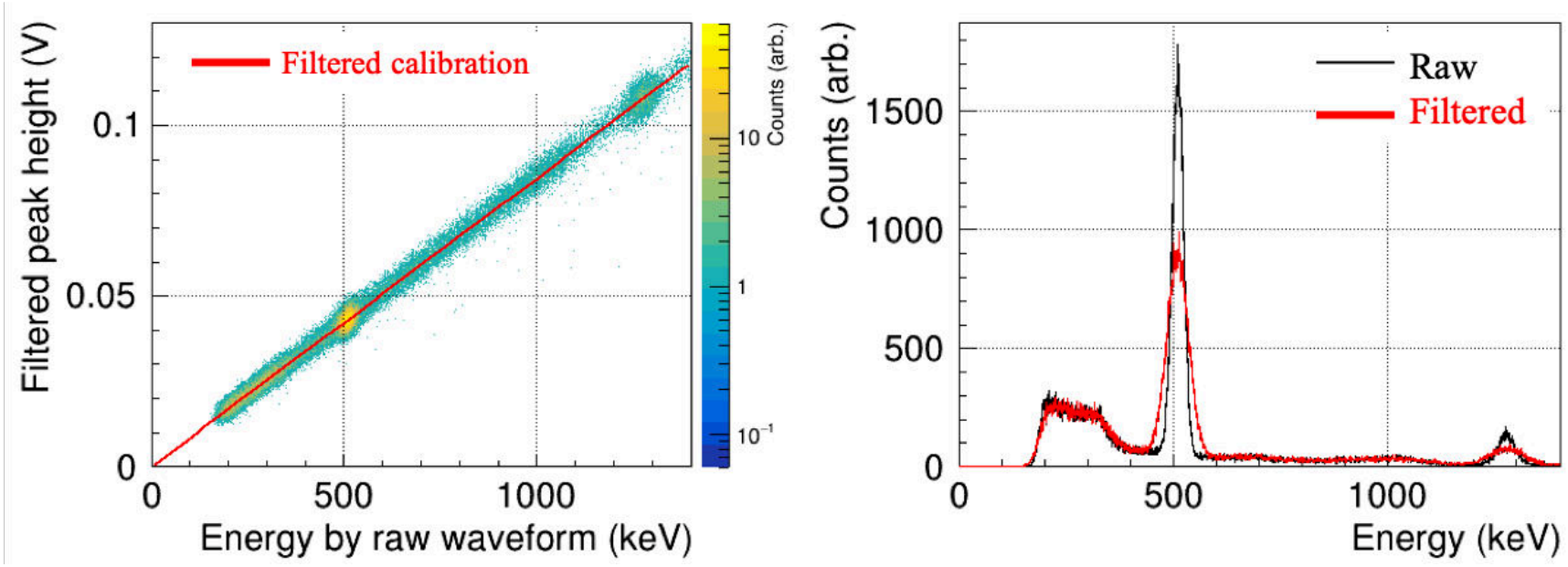

Figure 3.5: (Left) Correlation between filtered pulse peak heights and energy deposition estimated by integrating raw waveforms. (Right) Energy spectra. Good enough linearity and resolution were achieved.

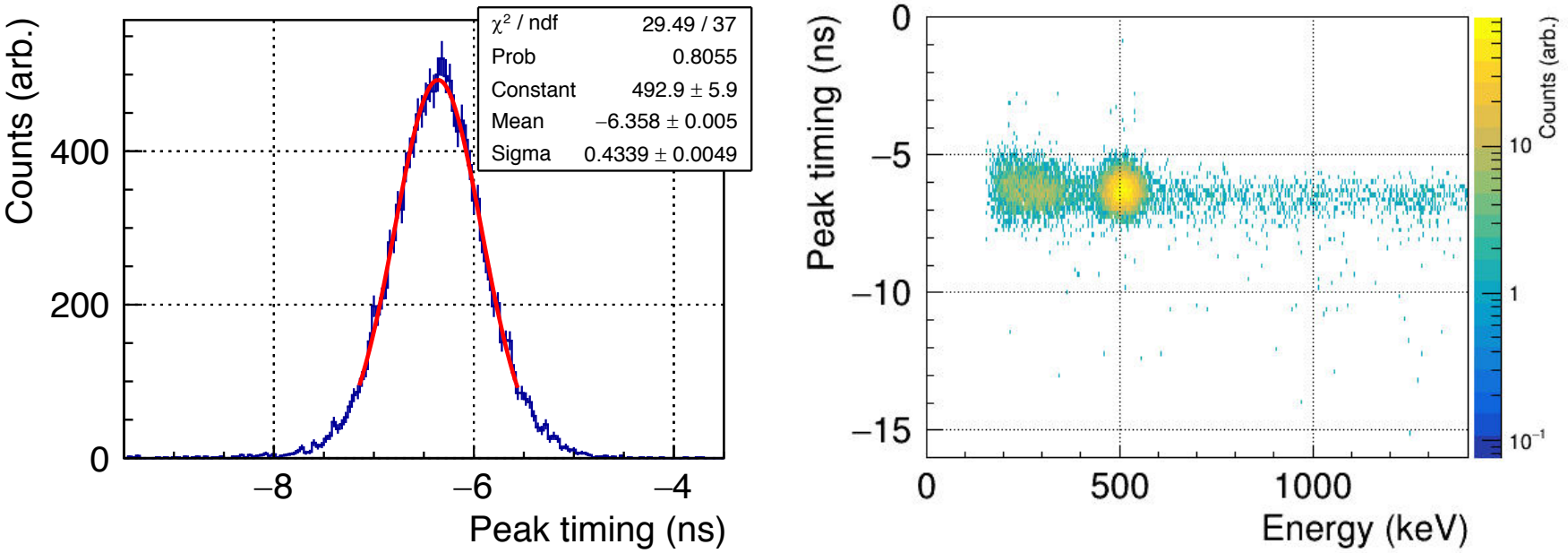

Figure 3.7: (Left) Timing spectrum of the filtered pulses' peak. (Right) Correlation between heights and timings. The timing resolution was as good as that evaluated by the raw waveforms.

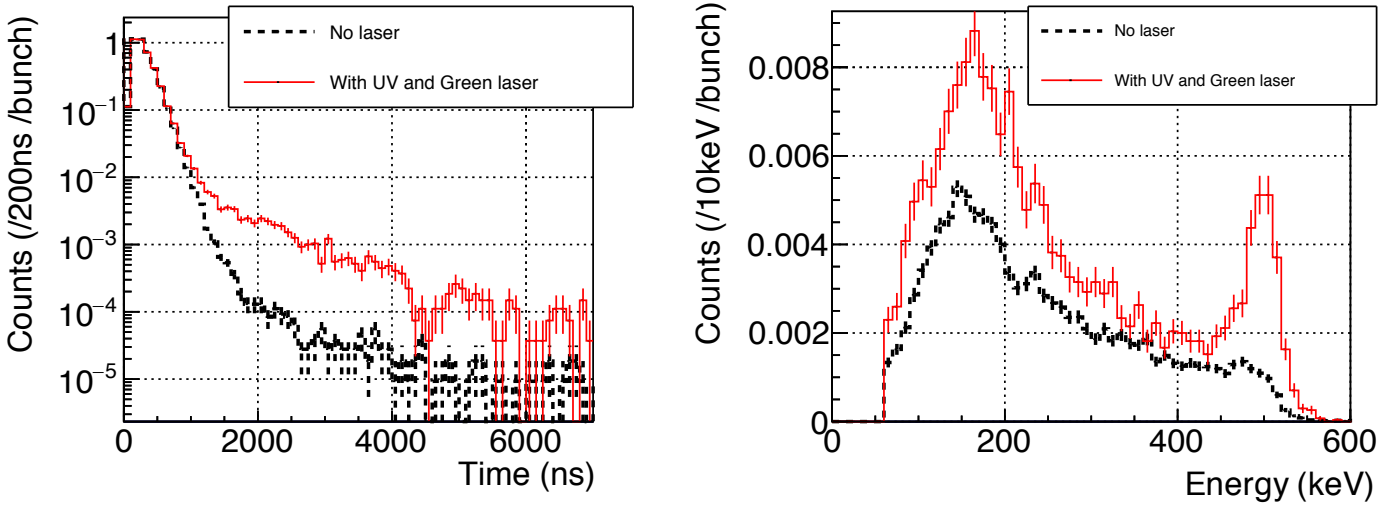

Figure 4.1: Timing (left) and energy (right) spectra of annihilation γ-rays from Ps excited in vacuum. An intensity of the very slow component after around 1000 ns increased by the laser irradiations. The decay mode of the slow component was confirmed to be the 2γ mode as expected.

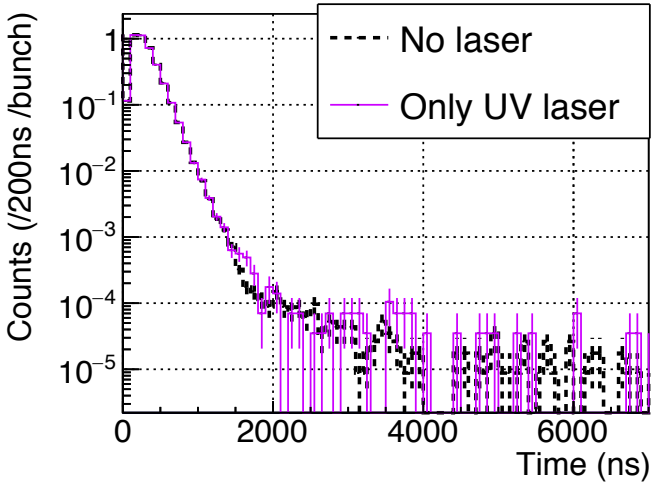

Figure 4.2: Timing spectrum by irradiating only UV laser on Ps in vacuum. The increase of the delayed component was not observed.

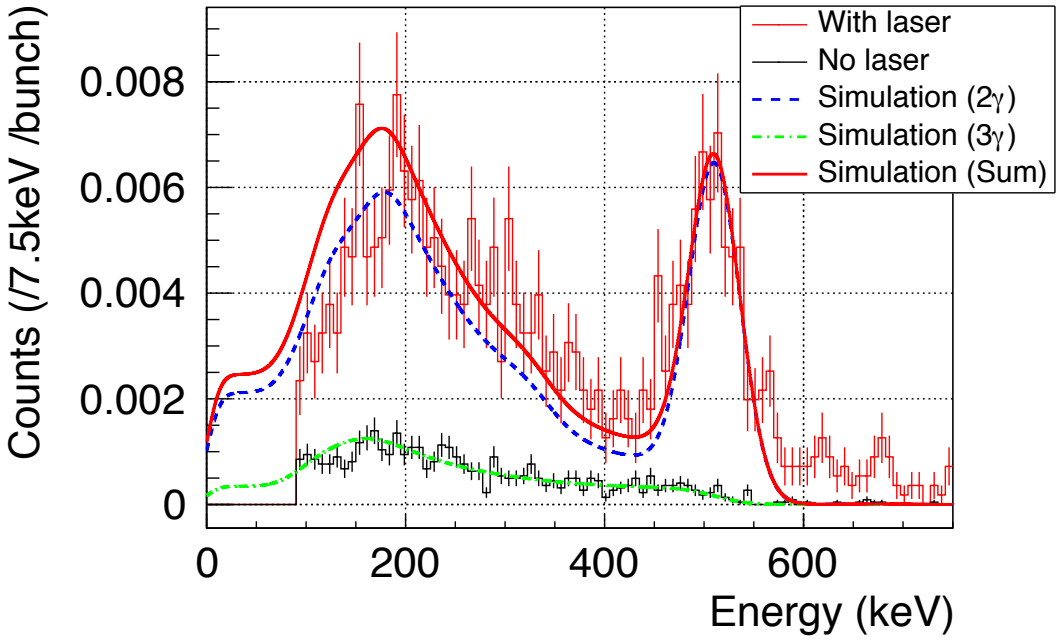

Figure 4.7: Energy spectra of γ-rays emitted around the laser irradiation. Because the total absorption peak of 511 keV γ-rays was clearly observed for the enhanced decay by the UV laser, it was assumed that the decay of 2P-Ps was fully in the 2γ mode.

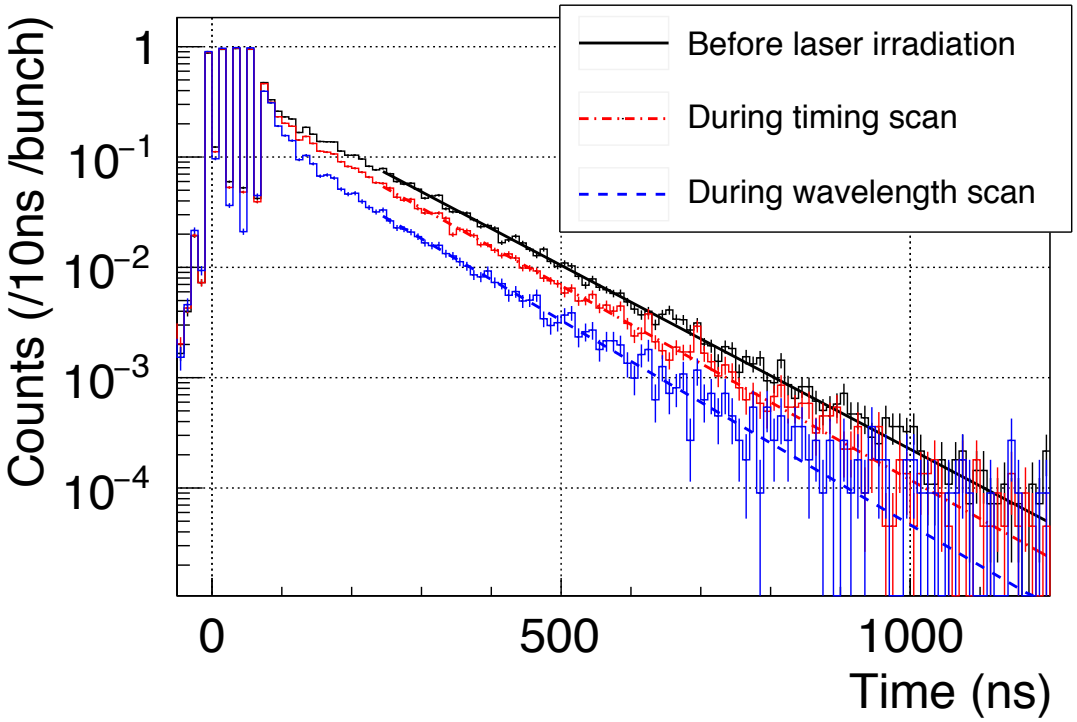

Figure 4.14: Timing spectra measured at different accumulations of the radicals. More radicals were accumulated during the wavelength scan, and they quenched o-Ps to reduce N_{oPs} and increased Γ_{po} by around 25 %.

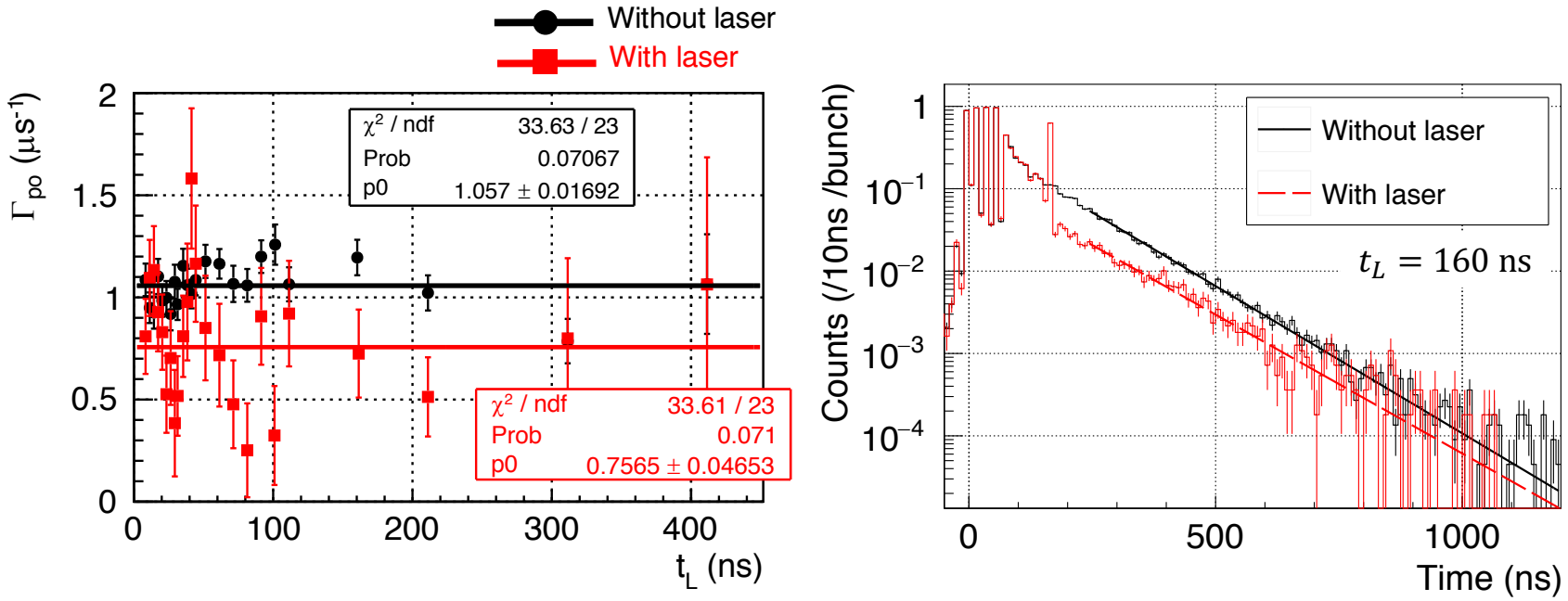

Figure 4.15: Decreases of the pick-off decay rates by energy selective 2P-Ps decay. (Left) Pick-off decay rates for various t_L. (Right) Example of the timing spectra. The spectrum was obtained with t_L = 160 ns. The less steep slope was observed with the laser. This is the result of the energy selective decay of 2P-Ps.

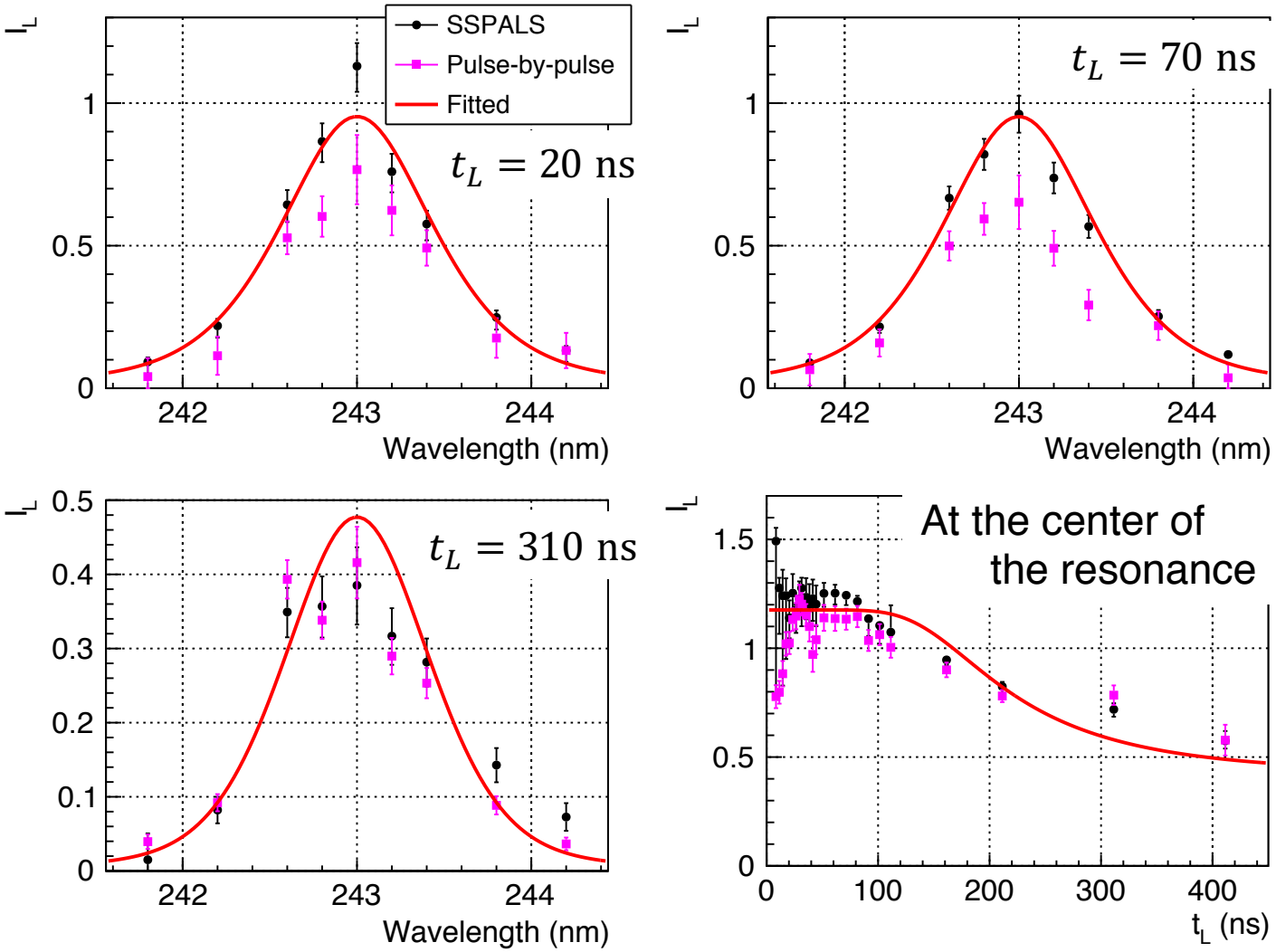

Figure 4.17: Comparisons of the resonance spectra and the timing dependence of I_L. Both results agreed at later t_L, and the same tendency of the dependence of Γ_2 on the kinetic energy was observed. Disagreements could be explained by inevitable systematic errors from the extrapolation in the pulse-by-pulse analysis.

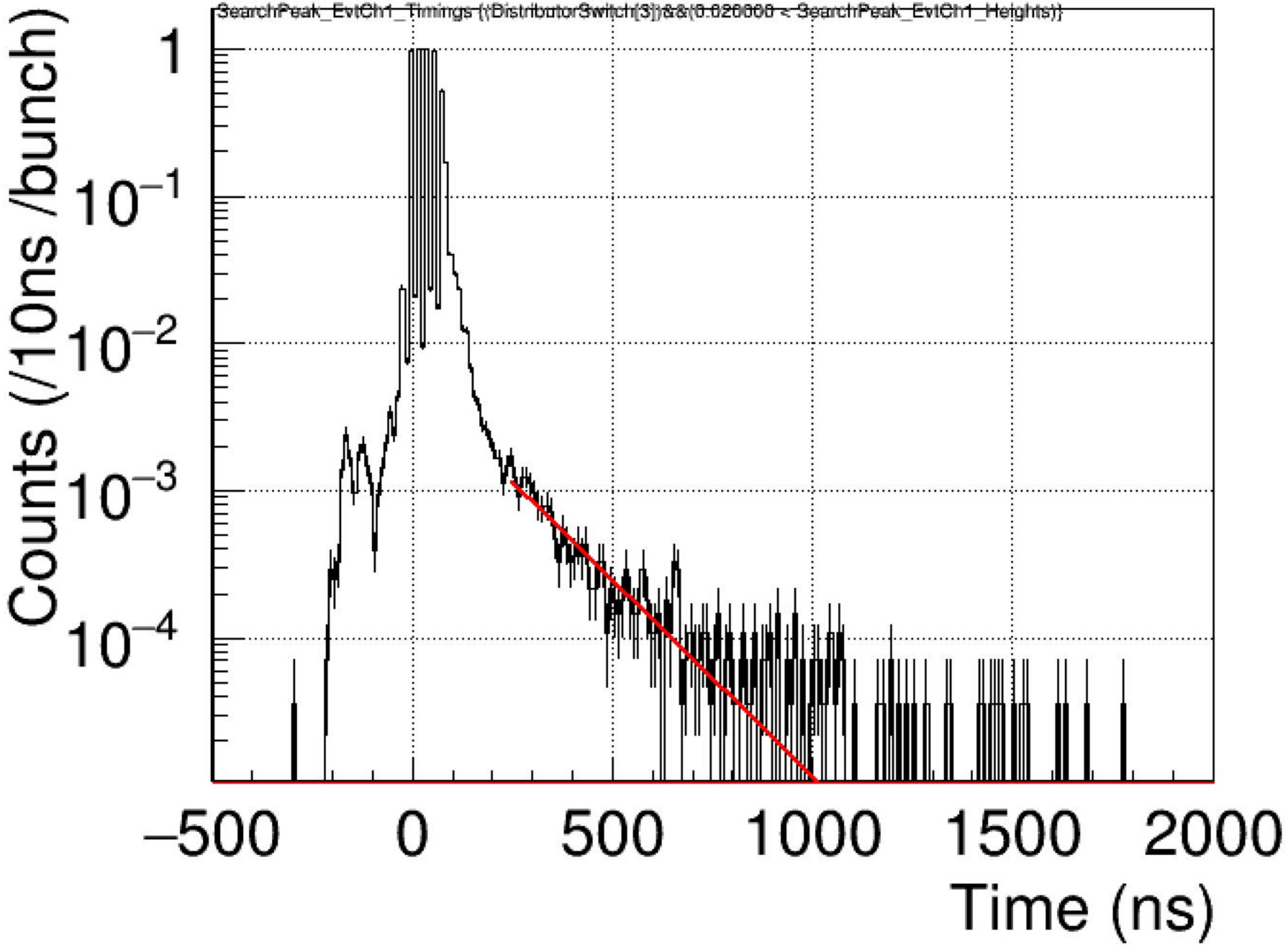
SearchPeak_EvtCh1_Timings (!DistributorSwitch[3]&&(0.020000 < SearchPeak_EvtCh1_Heights))
Counts (/10ns /bunch)
1
10^{-1}
10^{-2}
10^{-3}
10^{-4}
−500
0
500
1000
1500
2000
Time (ns)

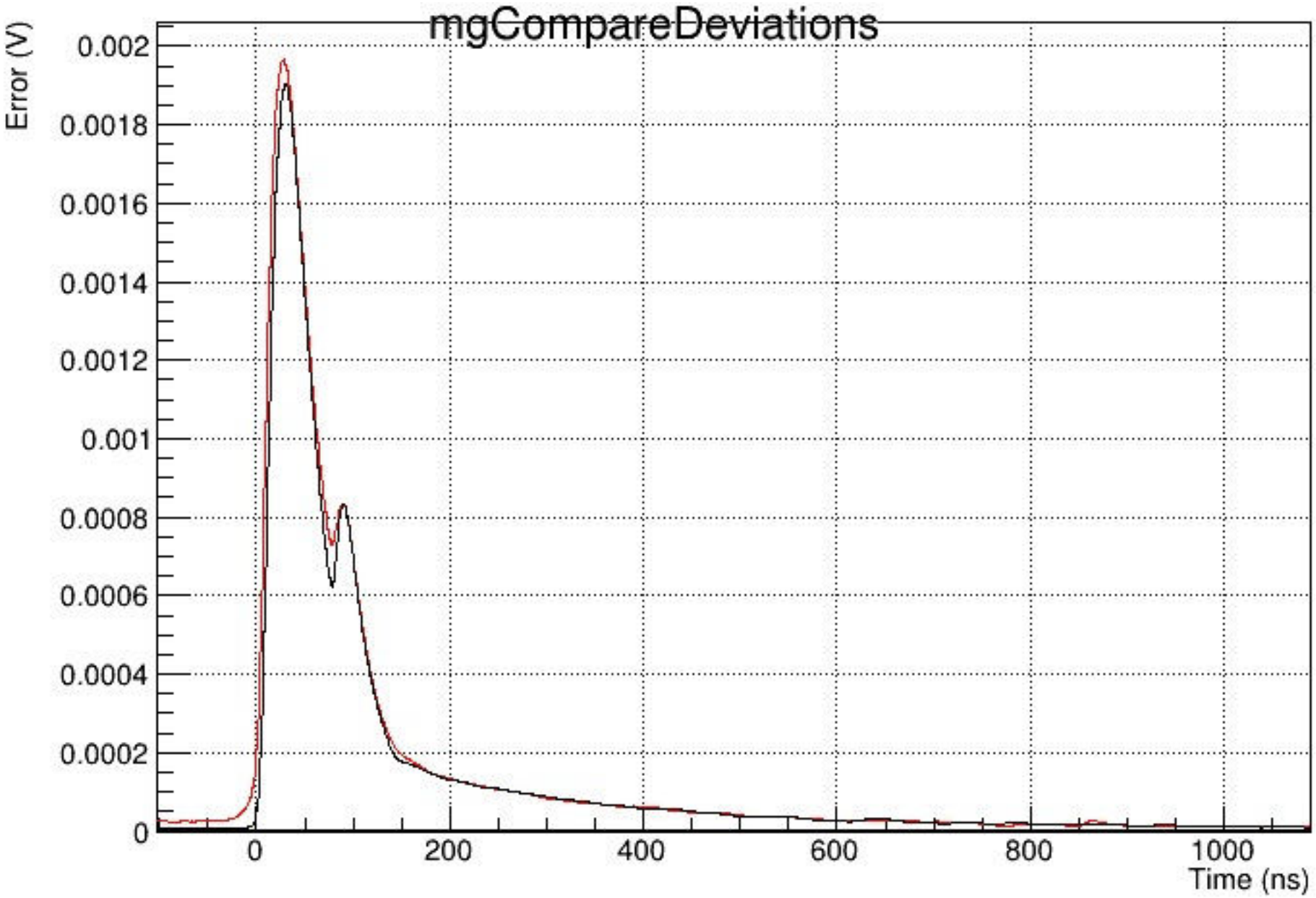
mgCompareDeviations
Error (V)
0.002
0.0018
0.0016
0.0014
0.0012
0.001
0.0008
0.0006
0.0004
0.0002
0
0
200
400
600
800
1000
Time (ns)

レーザーOFF 532nm Only
243nm Only 243nm and 532nm
486nm and 532nm

5月では長時間UV照射したため
最大6割程度まで生成率低下

mgIntensity_FullRange

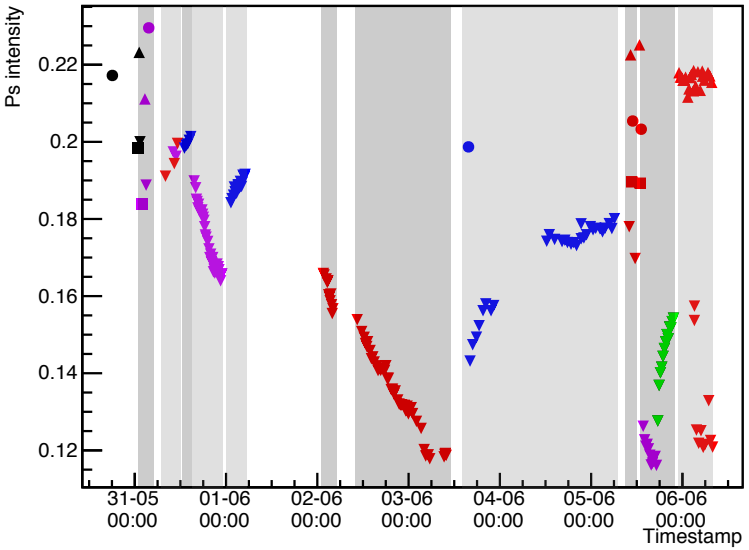

mgPsRatio_FullRange

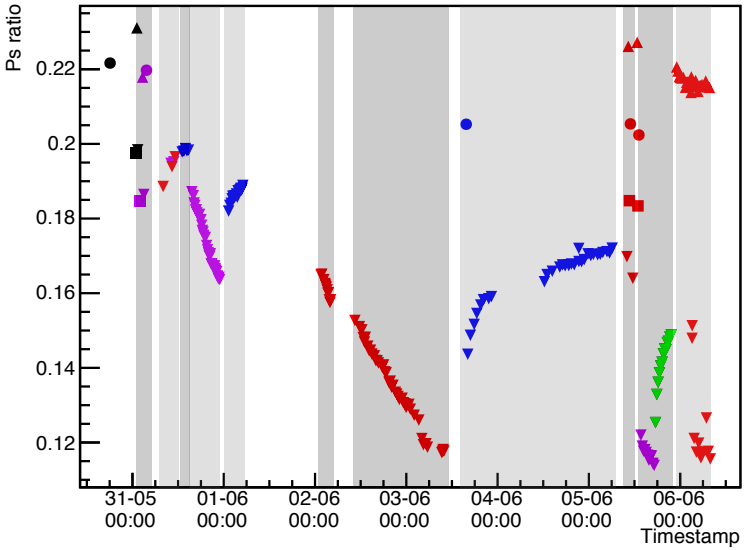

mgLife_FullRange

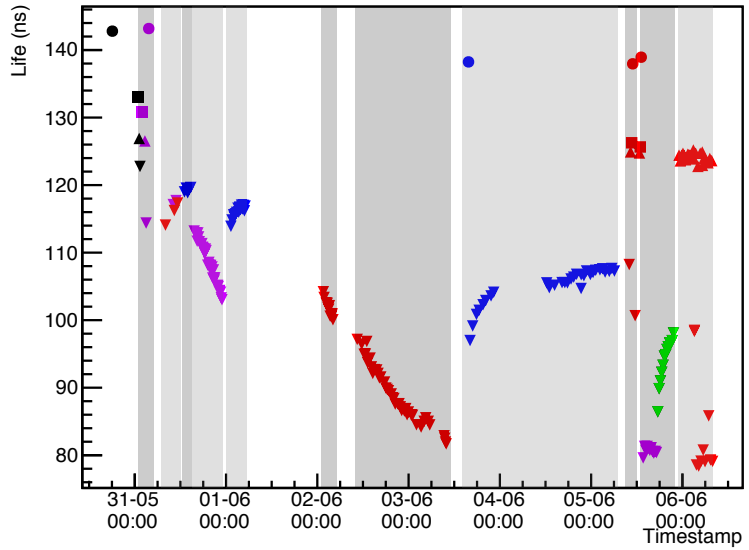

mgLifeVsRatio_FullRange

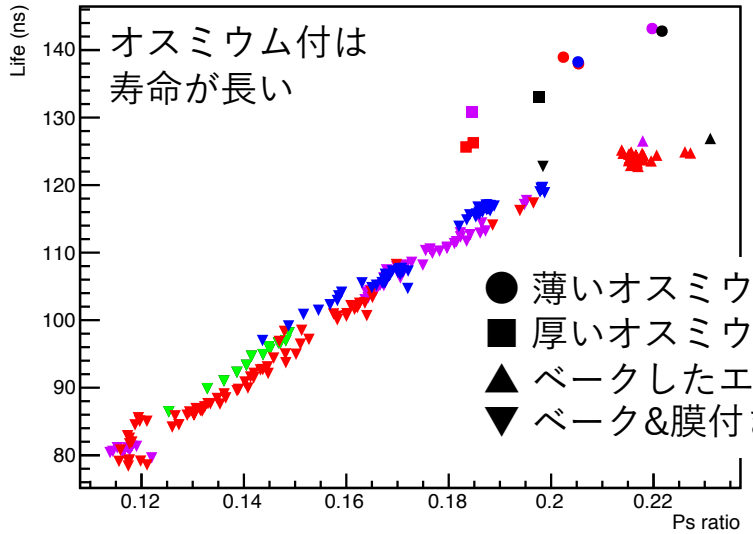

5月の実験

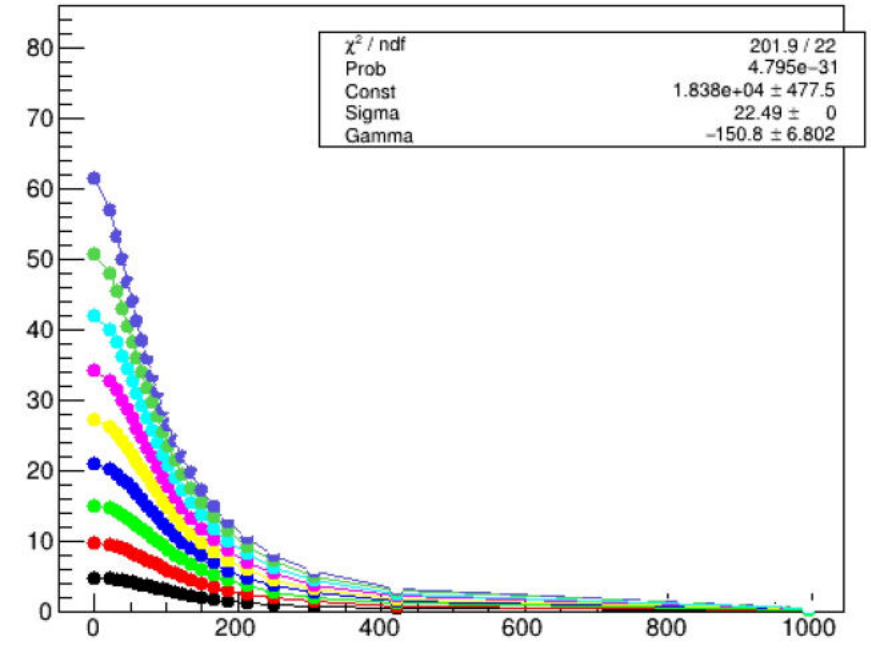
χ² / ndf 201.9 / 22
Prob 4.795e−31
Const 1.838e+04 ± 477.5
Sigma 22.49 ± 0
Gamma −150.8 ± 6.802
0
10
20
30
40
50
60
70
80
0
200
400
600
800
1000

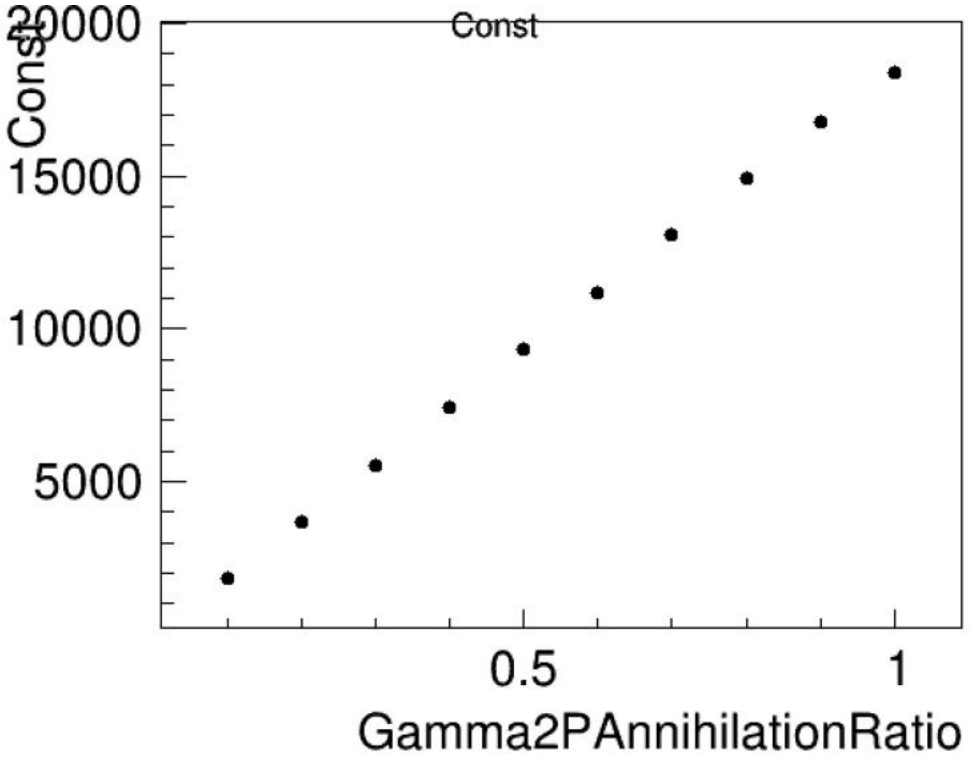
Const
Const
20000
15000
10000
5000
0.5
1
Gamma2PAnnihilationRatio